

## ORIGINAL ARTICLE

# The psychiatric disease risk factors DISC1 and TNIK interact to regulate synapse composition and function

Q Wang<sup>1,2</sup>, El Charych<sup>1,2</sup>, VL Pulito<sup>1</sup>, JB Lee<sup>3</sup>, NM Graziane<sup>3</sup>, RA Crozier<sup>1</sup>, R Revilla-Sanchez<sup>4</sup>, MP Kelly<sup>1,2</sup>, AJ Dunlop<sup>5</sup>, H Murdoch<sup>5</sup>, N Taylor<sup>6</sup>, Y Xie<sup>6</sup>, M Pausch<sup>1</sup>, A Hayashi-Takagi<sup>7</sup>, K Ishizuka<sup>7</sup>, S Seshadri<sup>7</sup>, B Bates<sup>6</sup>, K Kariya<sup>8</sup>, A Sawa<sup>7,9</sup>, RJ Weinberg<sup>10</sup>, SJ Moss<sup>4</sup>, MD Houslay<sup>5</sup>, Z Yan<sup>3</sup> and NJ Brandon<sup>1,2</sup>

<sup>1</sup>Pfizer Neuroscience Research Unit, Princeton, NJ, USA; <sup>2</sup>Pfizer Neuroscience Research Unit, Pfizer, Groton, CT, USA; <sup>3</sup>Department of Physiology and Biophysics, University at Buffalo, SUNY, Buffalo, NY, USA; <sup>4</sup>Department of Neuroscience, Tufts University School of Medicine, Boston, MA, USA; <sup>5</sup>Neuroscience and Molecular Pharmacology, Faculty of Biomedical and Life Sciences, University of Glasgow, Scotland, UK; <sup>6</sup>Pfizer Global Biotherapeutic Technologies, Cambridge, MA, USA; <sup>7</sup>Department of Psychiatry, Johns Hopkins University School of Medicine, Baltimore, MD, USA; <sup>8</sup>Department of Medical Biochemistry, Graduate School of Medicine, University of the Ryukyus, Okinawa, Japan; <sup>9</sup>Department of Neuroscience, Johns Hopkins University School of Medicine, Baltimore, MD, USA and <sup>10</sup>Department of Cell and Developmental Biology, University of North Carolina, Chapel Hill, NC, USA

**Disrupted in schizophrenia 1 (DISC1), a genetic risk factor for multiple serious psychiatric diseases including schizophrenia, bipolar disorder and autism, is a key regulator of multiple neuronal functions linked to both normal development and disease processes. As these diseases are thought to share a common deficit in synaptic function and architecture, we have analyzed the role of DISC1 using an approach that focuses on understanding the protein–protein interactions of DISC1 specifically at synapses. We identify the Traf2 and Nck-interacting kinase (TNIK), an emerging risk factor itself for disease, as a key synaptic partner for DISC1, and provide evidence that the DISC1–TNIK interaction regulates synaptic composition and activity by stabilizing the levels of key postsynaptic density proteins. Understanding the novel DISC1–TNIK interaction is likely to provide insights into the etiology and underlying synaptic deficits found in major psychiatric diseases.**

*Molecular Psychiatry* (2011) 16, 1006–1023; doi:10.1038/mp.2010.87; published online 14 September 2010

**Keywords:** DISC1; schizophrenia; synapse; TNIK

## Introduction

Schizophrenia, mood disorders and autism are severe debilitating psychiatric disorders with accumulating convergent evidence implicating dysfunction at the glutamatergic synapse.<sup>1–3</sup> Multiple genetic studies of schizophrenia and autism have highlighted genes whose products are found at synapses.<sup>4</sup> Post-mortem studies show altered expression of glutamate receptors in brains of patients with schizophrenia, major depression and bipolar disorder when compared with healthy individuals.<sup>5,6</sup> Likewise, the expression of PSD-95, a major scaffold protein at the postsynaptic density (PSD) of glutamate synapses, was decreased in the prefrontal cortex of schizophrenic brains.<sup>7</sup> Furthermore, molecular profiling using microarray and proteomic analyses on schizophrenia and bipolar

brains have revealed altered expression of other synaptic proteins, suggesting that synaptic deficits are associated with these disorders.<sup>8,9</sup>

Disrupted in schizophrenia 1 (DISC1) has emerged as a strong candidate gene for schizophrenia and other psychiatric disorders.<sup>10,11</sup> It was originally identified through study of a Scottish pedigree in which a balanced translocation between chromosomes 1 and 11 co-segregates with schizophrenia, bipolar disorder and recurrent major depression.<sup>12</sup> The name DISC1 was given to the gene disrupted at the breakpoint on chromosome 1.<sup>13,14</sup> Follow-up studies have reinforced the genetic association between variation in DISC1 and major mental illness, have highlighted links to brain structure and function<sup>10,15</sup> and have shown convergent genetic and biochemical links to other risk factors such as PDE4B (phosphodiesterase 4B).<sup>16,17</sup> In parallel with genetics, a rich biology for DISC1 function has begun to emerge,<sup>10,11,18</sup> with DISC1 implicated in cellular signaling, neuronal migration, axonal transport and neurogenesis in both the developing and adult brain.<sup>19–22</sup> The complexity of the biology is

Correspondence: Dr NJ Brandon, Pfizer Neuroscience Research Unit, Pfizer, East Point Road, Groton, CT 06340, USA.

E-mail: nick.brandon@pfizer.com

Received 15 February 2010; revised 18 July 2010; accepted 26 July 2010; published online 14 September 2010

highlighted by DISC1 being found in multiple subcellular locations and to bind to multiple protein partners.<sup>10,11</sup> The underlying molecular explanation for such diversity could be the neurodevelopmentally regulated expression or post-translational modification of different DISC1 isoforms, which could generate distinct protein complexes and/or target to distinct subcellular locations.<sup>10</sup> For example, DISC1 interacts with PDE4B in mitochondria and likely synapses to regulate cyclic adenosine monophosphate signaling,<sup>16,23</sup> with Ndel1 at the centrosome to regulate neuronal migration<sup>19,23</sup> and with glycogen synthase kinase 3 $\beta$  to modulate Wnt signaling in neural progenitors.<sup>21</sup> Together, these studies suggest that DISC1 is a multifunctional scaffold likely under exquisite spatial and temporal control, involved in different signaling pathways and of great importance for neuronal development and function.

We became very interested in understanding the role of DISC1 at the synapse after early reports localizing it to the PSD in human and rat brains as shown by electron microscopy and cellular fractionation techniques, respectively.<sup>24,25</sup> These observations were in line with our own predictions of a synaptic role for DISC1, which arose from *in silico* analysis of the 'DISC1 interactome', a DISC1 protein-protein interaction network based on yeast two-hybrid screening.<sup>26,27</sup> Our approach to study DISC1 function at the synapse was through the interrogation of DISC1-interacting proteins already known to be present in synapses. Within this effort we selected the Traf2 and Nck-interacting kinase (TNIK), a serine/threonine kinase from the Ste20 kinase family, for further study, as it was shown to bind DISC1, and had been found at the PSD in large-scale proteomic studies.<sup>28,29</sup> In recombinant systems, TNIK has been shown to regulate the actin cytoskeleton and c-Jun N-terminal kinase pathway<sup>30,31</sup> and, recently, was found to be an essential activator of Wnt target genes in the mouse small intestine.<sup>32</sup> The function of TNIK in the brain is poorly understood, but its potential importance in psychiatry has been highlighted by four independent studies implicating TNIK in either schizophrenia or bipolar disorder.<sup>33–36</sup> TNIK mRNA was shown to be upregulated in the dorsolateral prefrontal cortex of schizophrenia patients<sup>33</sup> and in lymphoblastoid cell lines from bipolar disorder patients when compared with their healthy monozygotic twins.<sup>34</sup> In addition, two single-nucleotide polymorphisms in TNIK were found to be associated with schizophrenia using functional neuroimaging as a quantitative phenotype in the context of a genome-wide association study.<sup>35</sup> Within the recent wave of genome-wide association study reports, a single-nucleotide polymorphism in TNIK was in the top 12 hits associated with schizophrenia in the African-American sample analysis from the MGS (Molecular Genetics of Schizophrenia) consortium.<sup>36</sup> These reports support a role for TNIK as a susceptibility gene for schizophrenia and related diseases, and, in conjunction with our DISC1-TNIK interaction

finding, suggested a functional role of TNIK and the DISC1-TNIK interaction in the brain.

In this study we show the importance of DISC1 and TNIK function in the regulation of key postsynaptic proteins, including glutamate receptors, PSD-95 and stargazin, with subsequent impact on synaptic activity. We demonstrate that TNIK is specifically expressed in neurons where it is highly enriched in the PSD, its expression profile mirrors that of DISC1 and DISC1 and TNIK interact in the brain. Using a combination of recombinant and neuronal cell models we show that DISC1 inhibits TNIK kinase activity. In primary neurons, we were able to modulate TNIK activity using both a peptide that inhibits TNIK kinase activity, derived from its binding site on DISC1, and small hairpin RNA (shRNA)-mediated knockdown to show that decreases in TNIK activity result in specific degradation of key postsynaptic molecules and changes in neuronal activity. Intriguingly, knockdown of DISC1 generates a predictable contrasting profile for the same postsynaptic proteins. These results identify TNIK as an important regulatory kinase at the PSD, which in turn is regulated by a physical interaction with DISC1. Understanding the importance of this protein interaction in disease will provide new insight into the synaptic deficits seen in a number of psychiatric diseases.

## Materials and methods

### Antibodies

The following primary antibodies were used in these experiments: monoclonal mouse-anti-TNIK (BD Biosciences, San Jose, CA, USA); rabbit anti-TNIK-N, pTNIKS764 and pTNIKS769 (Abgent, San Diego, CA, USA); and rabbit-anti-TNIK (Santa Cruz Biotechnology, Santa Cruz, CA, USA). Rabbit anti-DISC1 440 (DISC1-440) was generated in-house using antigenic peptide, H-[C]RTPHPPEEEKSPLQLQEW-D-OH, which is identical in human, mouse and rat. DISC1-440 consistently recognizes four major isoforms from rat brain lysates, including two bands at 130 kD and two around 100 kD. Anti-hemagglutinin (HA), Myc and green fluorescent protein (Santa Cruz); anti-synaptophysin (BD); anti- $\beta$ -actin (Sigma-Aldrich); anti-PSD95 (Sigma or Cell Signaling, Danvers, MA, USA); anti-GluR1, GluR2/3 and stargazin (Millipore, Billerica, MA, USA); anti-NR2b (Santa Cruz); and anti- $\beta$ -tubulin (Covance, Princeton, NJ, USA) were also used.

Secondary antibodies for western blot were Cruz Marker-compatible horseradish peroxidase-conjugated antibodies (Santa Cruz). Fluorescent secondary antibodies for immunofluorescence staining were Alexa Fluor 488 or 594 conjugated (Invitrogen, Carlsbad, CA, USA).

### Cell line and primary neuronal cultures

HEK293 and NIH3T3 cells were maintained in Dulbecco's modified Eagle's medium (Invitrogen) supplemented with 10% heat-inactivated fetal bovine serum (Invitrogen).

Rat hippocampal and cortical neuronal cultures were prepared from 18-day-old embryonic rats as previously described.<sup>37</sup> Briefly, hippocampi or cortices were dissociated by enzyme digestion with Papain Dissociation System (Worthington Biochemical, Lakewood, NJ, USA). Hippocampal cells were plated at 750 000 cells per dish and cortical cells at 2 000 000 cells per dish on poly-D-lysine-coated 60 mm dishes (BD). For imaging, hippocampal cells were plated as 30 000 cells per coverslip on poly-D-lysine/laminin-coated 12 mm coverslips (BD). All cells were plated and maintained in Neurobasal media (Invitrogen) supplemented with B27 and L-glutamine (Invitrogen) for 16–26 days *in vitro* (DIV). Half media was replaced with fresh growth media to feed cells every week till use.

#### Plasmid construction and transfection

Plasmids for the expression of HA-TNIK-WT, K54R (KM), ΔKD, CNH and ΔCNH, and EGFP-TNIK, and the expression of Myc-DISC1-WT and HA-DISC1-WT, 1–835, 1–801, 1–748, 1–726, 1–697, 1–597, 46–854, 150–854, 245–854, 291–854, 348–854 and 403–854 were described previously.<sup>19,31,38</sup> Plasmids for the expression of HA-DISC1-302–854, 313–854, 324–854 and 335–854 were generated by PCR-based subcloning. Plasmids for the expression of Myc-DISC1-ΔTNIK and AS1–6 were generated by site-directed mutagenesis using the Phusion Site-Directed Mutagenesis Kit (New England Biolabs, Ipswich, MA, USA). The constructs mentioned above are all human TNIK or DISC1. Mouse TNIK complementary DNA was cloned by reverse transcriptase-PCR from total mouse brain mRNA and subcloned into pCDNA3.1. The knockdown-resistant construct were generated by site-directed mutagenesis (see below for the knockdown target sequence). All oligonucleotides for PCR were synthesized by Invitrogen Custom Primers service. All restriction enzymes were from New England Biolabs.

For transfection of HEK293 and NIH3T3 cells, cells were seeded at 40–80% density and transfected 24 h later using Lipofectamine 2000 (Invitrogen). For primary neuronal culture transfection, hippocampal or cortical culture were plated at densities described above and transfected on 7–10 DIV with a Calcium Phosphate transfection kit or Lipofectamine (Invitrogen).

#### Peptides

The Tat membrane transduction domain peptide was from GenScript (Piscataway, NJ, USA). DISC1-pep-WT-tat, DISC1-pep-PM-tat and mouse/rat DISC1-pep-WT-tat were synthesized and purified by Alpha Diagnostic (San Antonio, TX, USA). All peptides were ordered in as lyophilized powders and dissolved in distilled water at a stock concentration of 1 mM. Unless specified elsewhere, 10 μM is the working concentration of peptides used in *in vitro* kinase assays and primary neuronal cultures. DISC1-pep-WT-tat was used in *in vitro* kinase assays, and mouse/rat DISC1-pep-WT-tat was used in rat primary neuronal cultures. Both

assays use Tat and DISC1-pep-PM-tat as controls (see Figure 4a for sequences).

#### Knockdown lentiviruses and lentivirus transduction

The vector used to generate shRNA plasmids was pLenti6-v5-D-TOPO (Invitrogen). TNIK knockdown lentiviruses were packaged by the Mission lentivirus packaging service provided by Sigma. The two specific target sequences for mouse and rat TNIK knockdown were: 5'-GAAGAACAAGCTCCGTGTGTA-3' (known as 806), and 5'-TGGATGGAGTGTATTATG CATA-3' (known as 807 and TNIK RNA interference (RNAi)). In the knockdown-resistant mouse TNIK construct, the target sequences were changed to: 5'-AAAAAACAACAACTAAGAGTATA-3' (806), and 5'-TGGACGGTGTATTCATGCAC-3' (807). The amino acid residues encoded by wild-type (WT) or mutated nucleotide sequences remained the same. Here, 801 is the empty vector control (also known as ctrl RNAi). Primary hippocampal neurons were transduced with knockdown lentiviruses on 7 DIV and harvested on 21 DIV when TNIK knockdown was >50%.

DISC1 knockdown lentiviruses were described previously.<sup>19,39</sup> The target sequence for mouse and rat DISC1 was: 5'-GGCAAACACTGTGAAGTGC-3' and the corresponding scramble control was 5'-GGAGCAGACGCTGAATTAC-3'.

#### In situ hybridization

Autoradiographic *in situ* hybridization was conducted with <sup>35</sup>S-labeled oligonucleotide antisense probes. Briefly, radioactive oligonucleotide probes specific for TNIK (mouse antisense: 5'-CTTGAAGAC CACCCTGACTATATTTCTGTGTGTTACC-3'; rat antisense: 5'-CTTGAAGACCACCCTCACTGTATTTCTGT GTGTTACC-3') or exon 2 of Disc1 (mouse antisense: 5'-TATGCCATCCATGGGCATCGGCCAGCCGCC CTGGTC-3') were hybridized to 20 μm sections and, after washing, slides were opposed to film for 14 days. Sense probes were tested in a similar manner and showed no signal. Similar patterns of expression were observed in mouse tissue with additional antisense probes corresponding to nucleotides 224–183, 940–901, 1119–1091 and 1238–1201 of TNIK (XM\_001473602.1) and to 161–121 of DISC1 (exon 2 of NM\_174854).

#### Immunofluorescence staining of brain slices

C57/BL6 male mice (8 weeks old) were deeply anesthetized and intracardially perfused with saline solution followed by 4% of paraformaldehyde. Brains were removed, post fixed overnight and cryoprotected in 30% sucrose. Free-floating sections were cut at 40 μm in a freezing microtome and kept at 20 °C in cryoprotective solution (30% sucrose, 30% ethylene glycol and 1% polyvinylpyrrolidone in phosphate-buffered saline (PBS)) until processing.

Sections were washed in PBS and incubated for 2 h in blocking solution (2% normal horse serum, 0.5% bovine serum albumin and 0.5% Triton X-100 in PBS) followed by incubation in blocking solution

containing the primary antibodies: rabbit anti-TNK1 (Abgent), goat anti-DISC1 (Santa Cruz) and mouse anti-NeuN (Millipore), all 1:500 for 72 h at 4 °C. After rinsing in PBS, sections were incubated in blocking solution containing secondary antibodies (anti-rabbit-Rhodamine Red X, anti-goat-fluorescein and anti-mouse-Cy5) for 2 h at room temperature, and then rinsed in PBS and mounted in slides. Sections were visualized using a Nikon confocal microscope.

#### *Immunofluorescence staining of primary neuronal cultures*

Cells on 12-mm poly-D-lysine/laminin-coated coverslips (BD) were washed with cold PBS and fixed with 4% paraformaldehyde in PBS for 10 min, followed by three washes with PBS and permeabilized with 0.2% Triton X-100 in PBS for 5 min. The coverslips were then blocked by the blocking buffer (5% normal donkey serum, 0.1% Tween 20 and PBS), followed by incubation with primary antibodies overnight in the blocking buffer. The coverslips were washed three times with 0.1% Tween 20 in PBS, 10 min each, followed by incubation with fluorescent secondary antibodies in the blocking buffer for 1 h. The coverslips were washed three times with 0.1% Tween 20 in PBS, 10 min each, and then mounted to glass slides (VWR) with Prolong Gold antifade reagent with 4,6-diamidino-2-phenylindole (Invitrogen). The coverslips were observed using Leica (Wetzlar, Germany) TCS SP5 confocal microscope ( $\times 63$ , oil).

For surface glutamate receptor 1 (GluR1) staining, cells were fixed in 4% paraformaldehyde/4% sucrose in PBS for 5 min and stained without permeabilization.

#### *Electron microscopy*

All procedures relating to the care and treatment of animals were in accordance with the institutional and National Institutes of Health guidelines. Pentobarbital-anesthetized (60 mg kg<sup>-1</sup> intraperitoneal) male Sprague-Dawley rats (3–5 months old, Charles River, Raleigh, NC, USA) were intracardially perfused with heparinized saline followed by 500 ml of fixative. Rats were fixed with 4% paraformaldehyde freshly depolymerized in phosphate buffer (0.1 M, pH 6.8) for light microscopy, or with a mixture of 4% paraformaldehyde and 1% glutaraldehyde in phosphate buffer for electron microscopy. Brains were postfixed overnight at 4 °C in the same fixative, cut at 40–50  $\mu$ m on a Vibratome and collected in cold phosphate buffer.

For pre-embedding electron microscopy, the basic procedure was identical except that sections fixed with glutaraldehyde were first treated with sodium borohydride (1% in PBS) to quench free aldehyde groups. After incubation with biotinylated secondary antibody, sections were incubated for 30 min with streptavidin Nanogold (1:100 dilution), rinsed in 0.2% sodium acetate and then silver intensified by 7-min incubation in IntenSE M reagents (GE Healthcare, Piscataway, NJ, USA) and rinsed again in sodium acetate. Reacted sections were postfixed 45 min in 1% osmium tetroxide in phosphate buffer;

after rinse in 0.1 M maleate buffer (pH 6.0), sections were incubated for 1 h in 1% uranyl acetate, then dehydrated through graded ethanol solutions, infiltrated with Spurr's resin, and heat-polymerized at 60 °C. Relevant chips from cortex and hippocampus were glued onto plastic blocks; thin sections (~80 nm) were collected on copper mesh grids and post-stained with uranyl acetate and Sato's lead. Control sections were processed in parallel in the absence of primary or secondary antibodies.

#### *Image analysis*

All confocal images were captured using identical acquisition parameters, defined as those that yielded optimal signal without saturation in control neurons. For measurements of surface GluR1 or PSD-95 immunoreactive puncta, confocal images were analyzed using Metamorph software (Molecular Devices, Downingtown, PA, USA). Only neurons exhibiting extensive dendritic spine formation were selected for analysis. For measuring punctate area and density, fluorescent images were thresholded such that pixels with grey values >120 (surface GluR1) and 130 (PSD-95) were binarized. For each neuron, regions of interest of 50  $\mu$ m length and 4  $\mu$ m width were drawn around three dendritic segments arising from the soma and analyzed using the Metamorph Integrated Morphometry Analysis tool. For average fluorescence intensity measurements, the same regions of interest detailed above were analyzed using the Metamorph Region Measurements tool without thresholding. All image analysis was performed blind of treatment conditions.

#### *Immunoprecipitation*

For preparation of cell extracts, HEK293 cells grown in six-well plates were washed once with ice-cold PBS. Cells were then lysed in 120–150  $\mu$ l of co-immunoprecipitation (co-IP) buffer (50 mM Tris-Cl (pH 7.5), 150 mM NaCl, 1 mM EDTA and 1% Triton X-100) with freshly add protease and phosphatase inhibitor cocktails (Sigma). After rocking for 30 min at 4 °C, cell lysates were collected by scraping and cleared by centrifugation at 12 000 g for 10 min at 4 °C.

For preparation of tissue extracts, freshly dissected rat brain tissues were cut to small pieces and immediately put into ice-cold co-IP buffer with protease and phosphatase inhibitors, followed by brief sonication. The tissue lysates were then rocked at 4 °C for 30 min and cleared by centrifugation at 12 000 g for 10 min at 4 °C. Another 5 min of centrifugation at 12 000 g was performed if lysates were still cloudy.

A total of 20  $\mu$ l of protein G-Sepharose 4 beads (GE Healthcare) equilibrated with co-IP buffer were mixed with 1–3  $\mu$ g of antibodies. After 1 h of incubation, the beads were washed one time with co-IP buffer, then mixed with cell or tissue lysates, and incubated 2 h to overnight at 4 °C with rocking. The beads were washed extensively with co-IP buffer to remove unbound proteins, separated by NuPage 4–12% Bis-Tris gels (Invitrogen) and subjected to western blotting.

### Crude membrane fractionation

Primary hippocampal neurons were homogenized in homogenization buffer (320 mM sucrose, 50 mM Tris-Cl (pH 7.5) and 1 mM EDTA) by passing through 26-gauge needles for 10 times, followed by centrifugation at 1000 g for 5 min. The supernatant was then spun at 45 000 r.p.m. for 1 h. The supernatant and pellet are cytosol and crude membrane fractions, respectively.

### Synaptosome and PSD fractionation of rat brain

The fractionation was performed as previously described.<sup>24</sup> Briefly, rat hippocampi or cortices were homogenized with a Teflon-glass homogenizer, followed by 1400 g centrifugation for 10 min to remove nuclei and unbroken cells and the supernatant was S1 and pellet P1. The S1 was centrifuged at 13 130 g for 10 min to yield S2 and crude synaptosomal pellet P2, which was further fractionated by discontinuous sucrose gradient centrifugation at 82 500 g for 2 h to yield ER-golgi membranes and synaptosomes. To prepare PSD fractions, the synaptosome fraction was extracted with Triton X-100, followed by centrifugation at 33 000 g for 20 min to yield supernatant TxS1 and pellet PSD1. The PSD1 was further extracted with Triton X-100 or Sarcosyl followed by centrifugation at 200 000 g for 20 min to yield supernatants TxP2 and SarS, and pellets PSD2 and PSD3.

### Full-length human TNIK purification

Suspension-adapted HEK293-EBNA cells in 1 l of freestyle 293 medium (Invitrogen) with 5% fetal bovine serum at 37 °C were transfected with 1 mg of TNIK-FLAG plasmid. At 18 h after transfection, the culture was transferred to a 31 °C incubator and allowed to incubate for additional 72 h. Cells were harvested by centrifugation at 900 g for 5 min.

In all, 0.5 l of cells were lysed in 150 ml 50 mM Tris pH 7.5, 100 mM NaCl, 50 mM NaF, 5% glycerol, 5 mM  $\beta$ -glycerophosphate, 1 mM Na orthovanadate, Complete protease inhibitor tablets EDTA-free (Roche, Indianapolis, IN, USA) and 6 mg per 100 ml AEBSF (4-(2-aminoethyl)benzenesulfonyl fluoride hydrochloride; Sigma). The lysate was cleared by centrifugation and the soluble protein was batch bound with 1 ml of FLAG resin (Sigma) rotating at 4 °C for 3.5 h. The FLAG resin was washed with 10 ml tris-buffered saline. TNIK was then batch eluted with 5 ml of elution buffer (tris-buffered saline, 0.1 mg/ml<sup>-1</sup> FLAG peptide (Sigma) and then run over a Superdex 200 size exclusion column (GE) in tris-buffered saline, 5% glycerol and 5 mM dithiothreitol. The elution fractions were pooled and frozen at -80 °C with 40% glycerol.

### In vitro kinase assays

Purified human TNIK was incubated with indicated peptides for 30 min on ice and the kinase reaction was carried out at 30 °C for 40 min in kinase buffer (50 mM Tris-Cl (pH 7.5), 5 mM MgCl<sub>2</sub>, 5 mM MnCl<sub>2</sub>, 5 mM dithiothreitol and 0.01% Triton X-100) with 5  $\mu$ M adenosine triphosphate (ATP), 5  $\mu$ Ci [ $\gamma$ -<sup>32</sup>P]-ATP and

2  $\mu$ g of myelin basic protein (MBP) as substrate in a 16  $\mu$ l reaction volume.

For IP kinase assays, TNIK was semi-purified from rat brain or cultured cells by IP as previously described. The protein G beads were extensively washed with co-IP buffer containing 700 mM NaCl and then equilibrated in the kinase buffer. The kinase reactions were carried out with 5  $\mu$ M ATP, 5  $\mu$ Ci [ $\gamma$ -<sup>32</sup>P]-ATP and 2  $\mu$ g of MBP as substrate in 40  $\mu$ l reaction volume with 20  $\mu$ l of protein G beads.

### Electrophysiology recordings

For DISC1 peptide treatment, miniature excitatory postsynaptic currents (mEPSCs) in cultured hippocampal neurons were recorded. Patch electrodes (3–5 M $\Omega$ ) were filled with the following internal solution (in mM unless specified): 130 Cs-methanesulfate, 10 CsCl, 4 NaCl, 1 MgCl<sub>2</sub>, 5 EGTA, 10 HEPES, 5 MgATP, 0.5 Na<sub>2</sub>GTP, 12 phosphocreatine, 20 leupeptin, 1 QX314, pH 7.2–7.3, 265–270 mosm l<sup>-1</sup>. The external solution consisted of (in mM unless specified): 127 NaCl, 5 KCl, 2 MgCl<sub>2</sub>, 2 CaCl<sub>2</sub>, 12 glucose, 10 HEPES, 0.5  $\mu$ M TTX, pH 7.4, 300 mosm l<sup>-1</sup>. Bicuculline (10  $\mu$ M) was added to the external solution to block GABA<sub>A</sub> receptors and AP-5 (50  $\mu$ M) was added to block N-methyl D-aspartate receptors. Recordings were obtained with an Axon Instruments 200B patch clamp amplifier that was controlled and monitored with an IBM PC running pCLAMP with a DigiData 1320 series interface (Axon instruments, Foster City, CA, USA). Electrode resistances were typically 2–4 M $\Omega$  in the bath. After seal rupture, series resistance (4–10 M $\Omega$ ) was periodically monitored. The cell membrane potential was held at -70 mV. The Mini Analysis Program (Synaptosoft, Leonia, NJ, USA) was used to analyze synaptic activity. For each different condition, mEPSC recordings of 8 min were used for analysis. Statistical comparisons of the amplitude and frequency of mEPSCs (mean  $\pm$  s.e.m.) were made using the Student's *t*-test.

For TNIK knockdown, mEPSCs were recorded in cultured rat hippocampal neurons (DIV 14–18) after transfection with control or TNIK knockdown shRNA constructs (ctrl RNAi and TNIK RNAi, respectively). In order to test whether the decrease in mEPSC amplitude could be restored, hippocampal neurons were co-transfected with TNIK RNAi and a TNIK construct resistant to knockdown (TNIK<sup>Resistant</sup>) or wild-type TNIK construct (TNIK<sup>WT</sup>). Statistical comparisons of the amplitude and frequency of mEPSCs (mean  $\pm$  s.e.m.) were made using the Student's *t*-test.

### Statistics

Unless specified elsewhere, Student's *t*-test was used to determine the statistical significance between two groups. MS Excel 2003 or GraphPad Prism 5 was used for data analysis and graph generation. Statistical significance was indicated by \**P* < 0.05, \*\**P* < 0.01 and \*\*\**P* < 0.001. Error bar indicates s.e.m.

**Results**

*A 13-amino acid region on DISC1 is required for its interaction with TNIK*

Previously, DISC1 and TNIK were reported to interact in a yeast two-hybrid screen, but the interaction was never confirmed in other systems.<sup>26</sup> In this study we show that HA-tagged TNIK and myc-tagged DISC1 are co-precipitated in a complex after coexpression in HEK293 cells (Figures 1a and b). Deletion of the kinase domain of TNIK (HA-TNIK ΔKD) abolished the interaction. However, kinase activity is not required for the interaction, as the kinase-dead mutant<sup>30</sup> (HA-TNIK K54R) retained the ability to interact with DISC1 (Figures 1a and b). Through similar co-IP assays with truncated N- and C-terminal DISC1 fragments, the binding site for TNIK was mapped to a 13-amino acid region, which extended from residue 335 to residue 347 on DISC1 (Supplementary Figure 1). Deletion of residues 329–350, as in the Myc-DISC1 ΔTNIK construct, led to the abolition of interaction with TNIK, which is consistent with the location of the binding site within the 335–347 region of TNIK (Figures 1c and d). Furthermore, alanine substitution (AS) mutants indicated that a three-amino-acid stretch (V336, L337 and R338) together with N344 on DISC1 are crucial for the interaction. DISC1 containing the mutation VLR336-338AAA (Myc-DISC1 AS1) only showed a weak interaction with TNIK, comparable to DISC1 ΔTNIK (Figures 1c and d). Identification of this binding site enabled us to

generate tools to dissect out a role for the DISC1–TNIK interaction (see below).

*DISC1 associates with TNIK in the brain*

TNIK protein is abundant in the brain and absent from most peripheral tissues in rats.<sup>40</sup> However, its specific localization and function in the brain are poorly characterized. Therefore, we utilized *in situ* hybridization, immunohistochemistry, immunofluorescence, electron microscopy and biochemical fractionation to determine the localization of TNIK in the brain and its relationship to the distribution of DISC1 (Figures 2a–e, Supplementary Figures 2a–d). The *in situ* hybridization showed that TNIK mRNA is expressed throughout the mouse brain, but appears to be particularly high in the dentate gyrus of hippocampus and the cerebellum, with significant levels in the cortex, very similar to the pattern shown for DISC1 (Figure 2a). TNIK mRNA was also observed in similar regions of rat brain (Supplementary Figure 2a). The hippocampus and cortex are critical anatomical substrates in schizophrenia, and hence we focused our subsequent experiments on these regions. Immunohistochemistry of mouse brain sections showed colocalization of DISC1 and TNIK in projections in the CA1 of hippocampus (Figure 2b) and the somatosensory cortex (Supplementary Figure 2b). Immunofluorescence labeling of primary hippocampal cultures showed that TNIK colocalizes with the neuronal marker MAP2 (microtubule-associated protein 2), but not with the glial marker, glial fibrillary

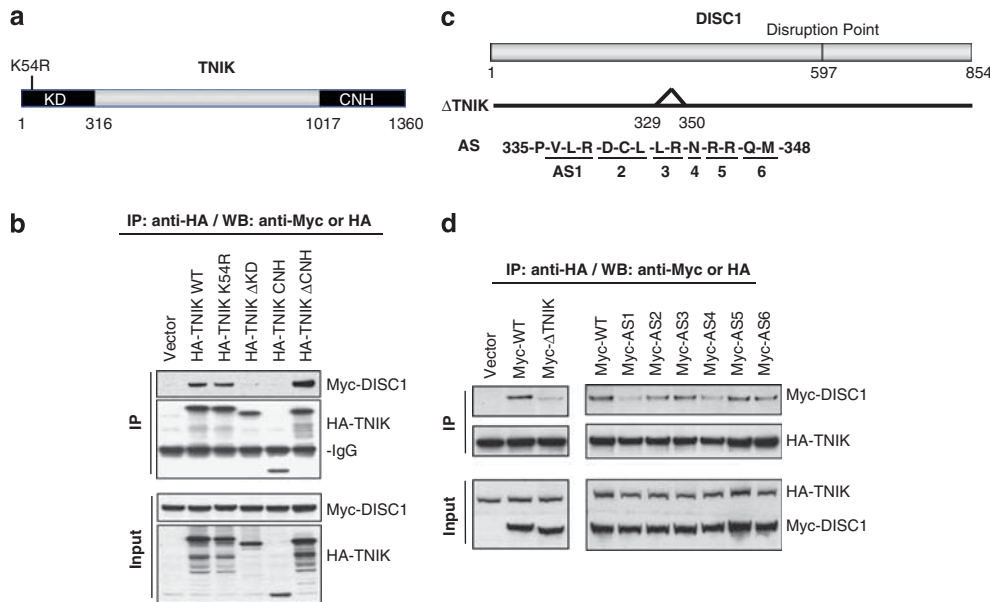


**Figure 1** A 13-amino acid region on DISC1 is required for its interaction with TNIK. **(a)** Schematic representation of TNIK with the N-terminal kinase domain (KD) and C-terminal citron homology domain (CNH). The point mutant K54R is a kinase-dead mutant. **(b)** DISC1 binds to the kinase domain of TNIK. Myc-DISC1 co-immunoprecipitates with HA-TNIK WT but not HA-TNIK ΔKD from HEK293 cells. **(c)** Schematic representation of DISC1 and point mutants within the TNIK binding site. Amino acids 329–350 are deleted in DISC1 ΔTNIK. DISC1 AS1–6 are alanine substitution (AS) mutants with the underlined amino acid residues mutated to alanine. **(d)** Amino acids crucial for the interaction of DISC1 and TNIK. Myc-DISC1 WT, but not myc-DISC1 ΔTNIK, co-immunoprecipitates with HA-TNIK from HEK293 cells.

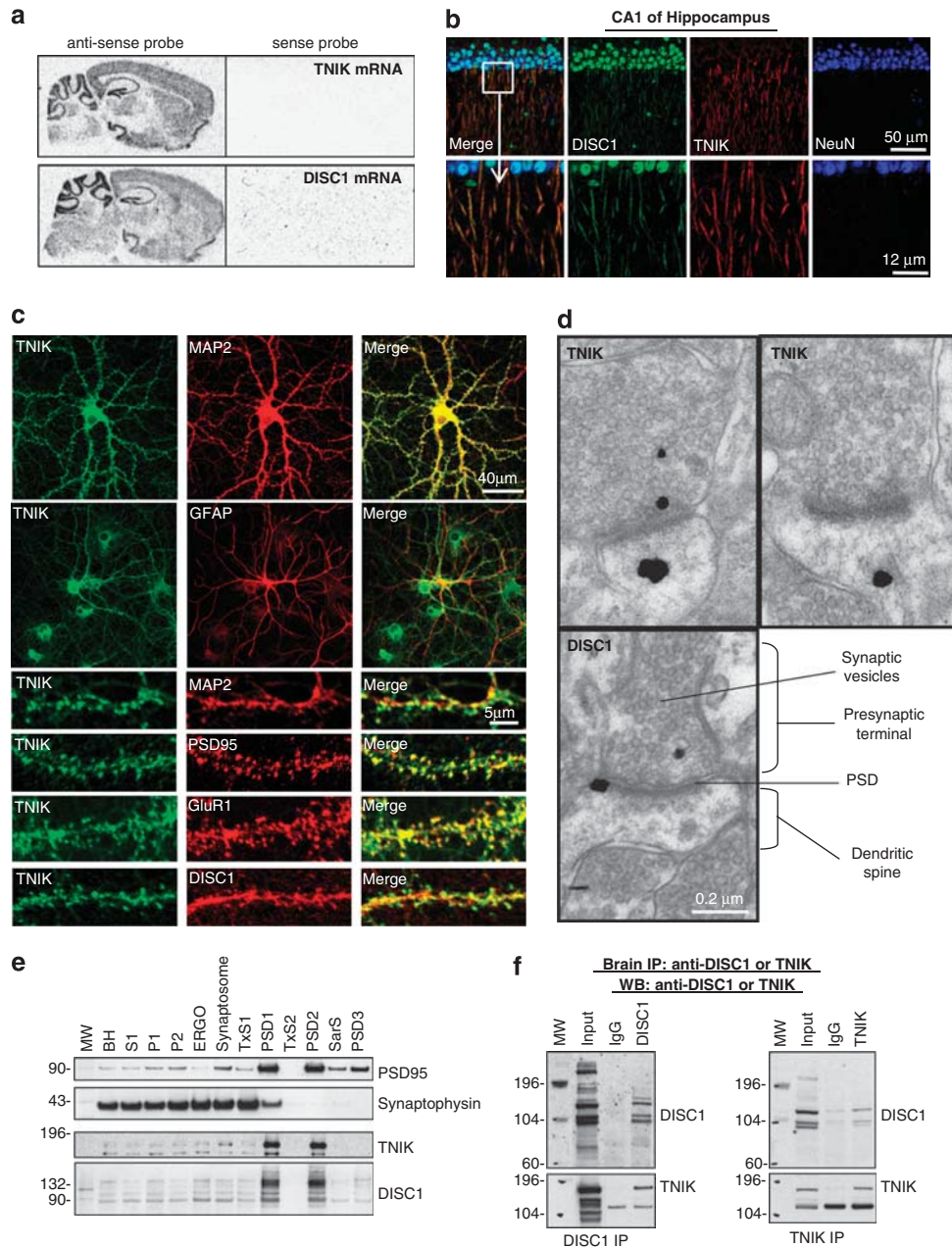


**Figure 2** DISC1 associates with TNIK in the brain. **(a)** Expression of TNIK and DISC1 mRNA in adult mouse brain shown by *in situ* hybridization. **(b)** Single plane confocal images of CA1 from adult mice immunostained for DISC1 (green), TNIK (red) and the neuronal marker NeuN (blue) showing colocalization of DISC1 and TNIK in likely dendritic projections. **(c)** Single plane confocal images of 19–26 DIV rat primary hippocampal cultures showing colocalization of TNIK with neuronal and PSD markers and DISC1, but not with the glial marker, glial fibrillary acidic protein (GFAP). **(d)** Electron micrographs, with pre-embedding immunogold staining, showing the presence of TNIK and DISC1 in adult rat CA1 dendritic spines. **(e)** TNIK and DISC1 are enriched in PSD fractions from rat hippocampi. BH, brain homogenate; ERGO, ER and Golgi apparatus; P1, nuclei and unbroken cells; P2, organelles; PSD1–3, PSD fractions 1–3; S1, cytoplasm; SarS, Sarcosyl soluble fraction; TxS1 and 2, Triton X-100 soluble fractions 1 and 2. **(f)** Co-immunoprecipitation of TNIK and DISC1 from rat brain. IPs were performed with DISC1-440 (left) and TNIK Santa Cruz (Right) antibodies, followed by western blotting (WB) using both antibodies.

acidic protein, indicating that TNIK is specifically expressed in neurons (Figure 2c). More specifically, the punctate staining of TNIK colocalized extensively with the puncta of PSD-95 and the AMPA receptor subunit GluR1, suggesting that TNIK is found at

excitatory synapses (Figure 2c). Critically, TNIK also colocalized with DISC1 dendritic puncta in primary hippocampal neurons (Figure 2c). Electron microscopy provided further evidence that TNIK is present in dendritic spines and localized both to pre- and

postsynaptic compartments, with enrichment in the latter (Figure 2d). This pattern is very similar to that observed for DISC1 (Figure 2d).

The postsynaptic localization of TNIK was confirmed biochemically after fractionation of rat hippocampi, which showed TNIK to be greatly enriched in PSD fractions, alongside DISC1 (Figure 2e and Supplementary Figure 2d). Most importantly, endogenous TNIK and DISC1 specifically co-immunoprecipitate from rat brain, utilizing either a DISC1 (Figure 2f, left) or TNIK (Figure 2f, right) antibody to isolate the complex. Together, colocalization and co-IP of endogenous TNIK and DISC1 proteins provide convincing evidence that DISC1 interacts with TNIK in the brain and implicate the PSD as a major functional site for these complexes.

*DISC1 inhibits the kinase activity of TNIK in cells*

To determine whether DISC1 regulates TNIK kinase activity, we utilized a cell rounding assay, which was previously shown to be dependent on TNIK kinase activity.<sup>30</sup> Expression of TNIK in Phoenix-A, NIH3T3 and Hela cells results in the disruption of F-actin structure and inhibition of cell spreading.<sup>30</sup> This was shown to be dependent on the kinase activity, as a kinase-dead mutant, TNIK K54R, did not cause this effect.<sup>30</sup> NIH3T3 cells were transfected with TNIK WT or TNIK K54R alone. As expected, expression of TNIK WT induced cell rounding, whereas cells expressing TNIK K54R exhibited a regular morphology comparable to neighboring non-transfected cells (Figure 3a and Supplementary Figures 3a and b). Expression of DISC1 WT alone did not alter cell spreading or

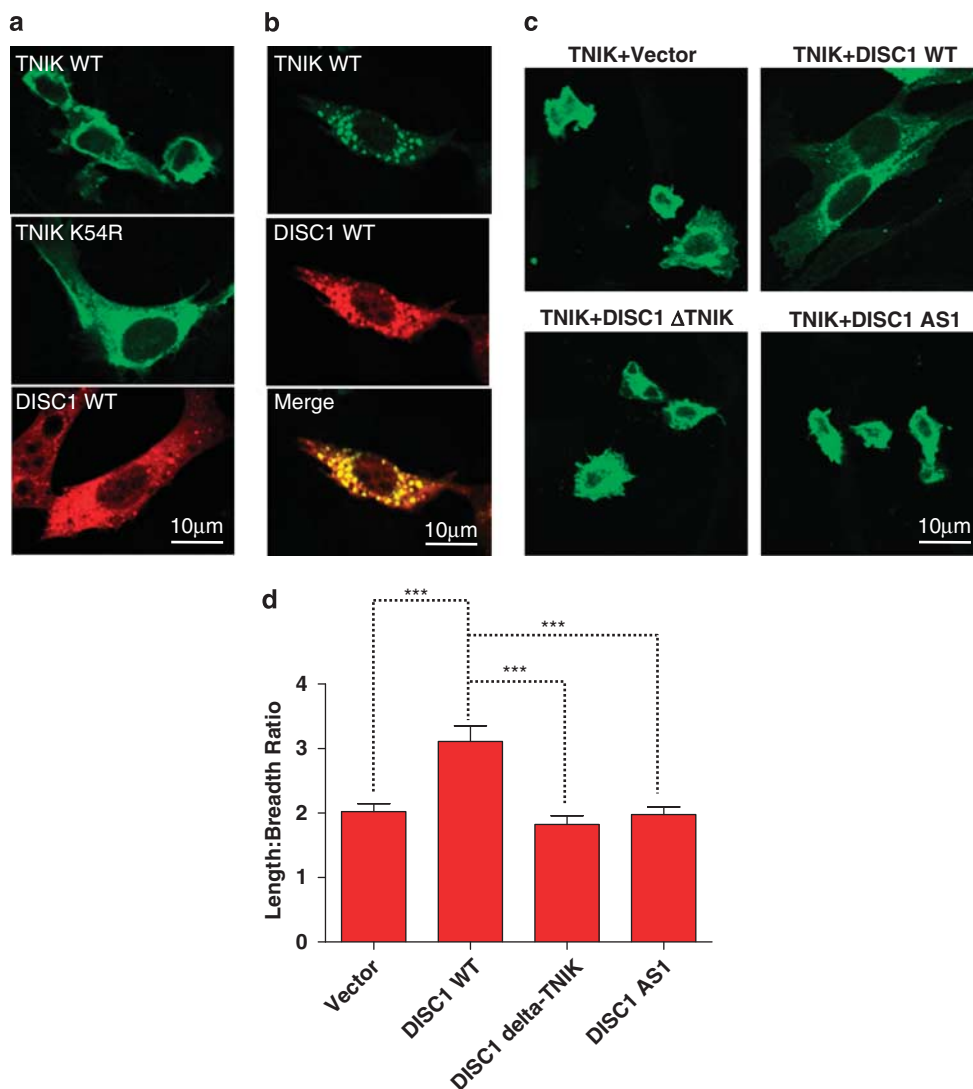


**Figure 3** DISC1 inhibits TNIK kinase activity-dependent cellular outputs. (a) Kinase-dependent cell rounding induced by TNIK. NIH3T3 cells were transfected with HA-TNIK WT, K54R or Myc-DISC1 WT alone, followed by immunofluorescence staining with anti-HA or anti-Myc antibody. (b) DISC1 inhibits TNIK-induced cell rounding. NIH3T3 cells were co-transfected with HA-TNIK WT and Myc-DISC1 WT followed by immunofluorescence staining with anti-HA and anti-Myc antibodies. (c) The TNIK binding site on DISC1 is required for inhibition of TNIK-induced cell rounding. Representative images of cells with indicated co-transfection and stained for HA-TNIK, and the length-to-breadth ration of cells were analyzed in (d) as a surrogate measure of cell spreading.  $N > 30$ . \* $P < 0.05$ , \*\* $P < 0.01$ , \*\*\* $P < 0.001$ .

morphology, with DISC1 exhibiting a strong punctate staining in the cytoplasm and weak staining in the nucleus, consistent with previous observations<sup>41</sup> (Figure 3a and Supplementary Figure 3a). Remarkably, when TNIK was co-transfected with DISC1, it was unable to induce cell rounding (Figure 3b and Supplementary Figure 3a). Furthermore, TNIK was found to be colocalized with DISC1 at cytoplasmic puncta (Figure 3b and Supplementary Figure 3a).

To further determine the specificity of the inhibition, TNIK was co-transfected with either empty vector or DISC1 WT. We also tested DISC1  $\Delta$ TNIK, or DISC1 AS1, whose interaction with TNIK was abolished by these mutations (Figures 1c and d). As TNIK staining overlaps with F-actin cytoplasmic staining in NIH3T3 cells, it can be objectively used to reflect the morphology of a cell (Supplementary Figures 3 and 4). Therefore, the length-to-breadth ratio of a cell, as determined from TNIK staining, was used as a surrogate measure of cell rounding (Figures 3c and d and Supplementary Figure 4). Consistent with the protein–protein interaction results, DISC1 WT significantly increased the average length-to-breadth ratio of a cell, compared with the empty vector control and the two non-binding mutants, DISC1  $\Delta$ TNIK and DISC1 AS1, when co-expressed with TNIK (Figures 3c and d). These results indicate that the interaction of DISC1 with TNIK is required for the inhibition of TNIK kinase activity. As DISC1 binds to the kinase domain of TNIK, we suggest that DISC1 may directly inhibit kinase activity, but cannot rule out an effect through regulating the subcellular localization of TNIK.

#### *The binding site-derived DISC1 peptide inhibits TNIK kinase activity*

To study the function of the TNIK–DISC1 interaction in neurons, we synthesized a 21-mer peptide conjugated to the membrane transduction domain of Tat, whose sequence reflected the region of DISC1 that contains the residues critical for the interaction with TNIK (Figures 1c and d and Supplementary Figure 1). We hypothesized that this 32-mer peptide, known as DISCpep-WT-tat, would enter cells so as to disrupt specifically the interaction of DISC1 and TNIK and/or inhibit the kinase activity of TNIK. As controls, we also synthesized the 11-mer Tat membrane transduction domain peptide and a related 32-mer tat-conjugated peptide known as DISCpep-PM-tat (point mutation) where the sequence is mutated to VLR336-338AAA (AS1) that does not interact with TNIK (Figures 1c and 4a).

We hypothesized that the DISCpep-WT-tat peptide might ablate the interaction between DISC1 and TNIK *in vitro*. However the DISCpep-WT-tat peptide or the tat control peptide was unable to disrupt the DISC1 and TNIK interaction, as shown by co-IP from HEK293 cells or from rat brain. We attempted to competitively disrupt the interaction by performing the co-IP in the presence of peptides (Supplementary Figure 5). We conclude that the interaction between DISC1 and TNIK cannot be disrupted by DISCpep-

WT-tat peptide, because it is of such high affinity, because the conformation of the peptide is such that it cannot mimic a surface able to interact with DISC1, or because of additional binding sites.

As DISC1 inhibits the kinase activity of TNIK in cells, we wondered whether the DISCpep-WT-tat peptide might behave similarly as the whole DISC1 protein, as this would provide a means of both evaluating whether this peptide interacted with TNIK and whether this region contributed to the observed inhibitory effect that DISC1 exerts on TNIK activity. These peptides were tested in an *in vitro* TNIK kinase assay using MBP as substrate (Supplementary Figure 6a) and purified human TNIK. DISCpep-WT-tat strongly inhibited the kinase activity of TNIK, compared with reactions without peptide or with Tat control peptide (Figures 4b and c). The DISCpep-PM-tat peptide only showed marginal inhibition of MBP phosphorylation compared with Tat, suggesting that the three mutated amino acid residues are crucial for efficient inhibition of TNIK (Figures 4b and c). This result is consistent with the data that DISC1 AS1 could not inhibit TNIK in cell-based assays (Figures 3c and d). Similar to many other kinases, autophosphorylation enhances the kinase activity of TNIK (Supplementary Figure 6b). To determine if the DISCpep-WT-tat peptide is also able to inhibit TNIK in its autophosphorylated state, kinase assays were performed with TNIK after a pre-autophosphorylation step. DISCpep-WT-tat showed an inhibition profile similar to that observed with the non-auto phosphorylated form of TNIK (Figures 4b and c). To determine if DISCpep-WT-tat also inhibits TNIK in complex with its interactors, endogenous TNIK was immunoprecipitated, under mild conditions that preserve binding to a range of interacting partners (Q Wang and NJ Brandon, unpublished), from HEK293 cells or 22DIV rat hippocampal cultures, followed by a kinase assay using MBP as substrate (Figures 4d and e). DISCpep-WT-tat strongly inhibits the kinase activity of endogenous TNIK as well as purified TNIK (Figure 4). It is worth noting that TNIK from neuronal cultures is much more active than TNIK from HEK293 cells, although more TNIK was immunoprecipitated from HEK293 cells. This suggests that the kinase activity of TNIK is dependent on the cellular environment from which it is isolated.

These data, together with the cell rounding assay, provide strong evidence that DISC1 is a negative regulator of TNIK kinase activity. Importantly, we have developed a DISC1 sequence-based peptide tool that inhibits TNIK kinase activity and will allow further analysis of TNIK activity in neurons.

#### *The inhibitory DISC1 peptide leads to dephosphorylation of TNIK and reduction in TNIK protein level*

The rat version of peptide DISCpep-WT-tat was introduced into rat primary hippocampal cultures as a specific inhibitor of TNIK, using Tat and DISCpep-PM-tat as control peptides (Figure 4a). Unfortunately,

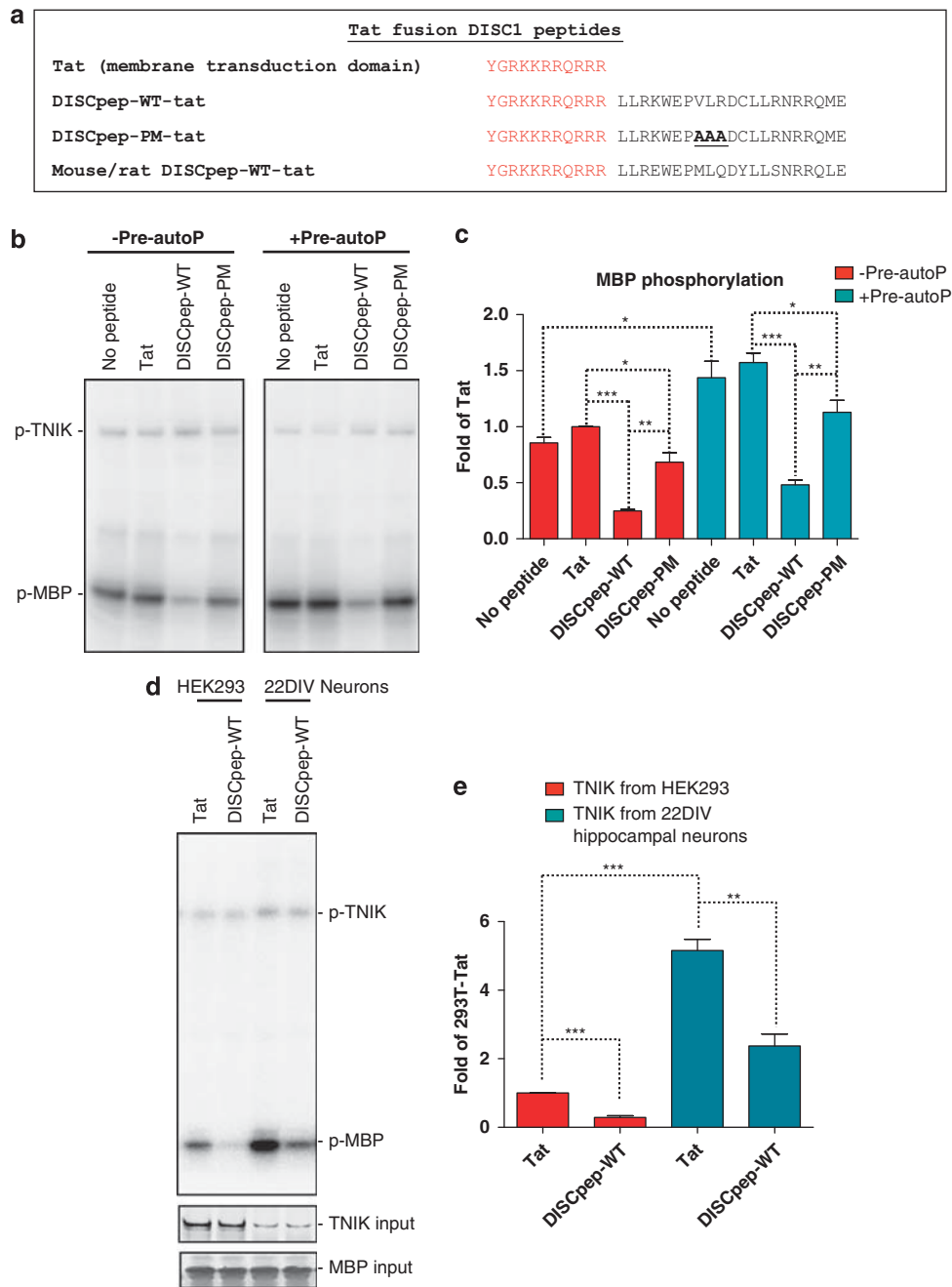


**Figure 4** The binding site-derived DISC1 peptide inhibits TNIK kinase activity. **(a)** Sequences of DISC1 peptides fused with the membrane transduction domain of Tat. DISCpep-WT contains amino acids 329–349 of human DISC1 and DISCpep-PM has three residues substituted by alanine. Mouse/rat version of DISCpep-WT contains amino acids 330–350 in mouse DISC1 and is 100% identical in mouse and rat. **(b)** DISCpep-WT inhibits kinase activity of TNIK *in vitro*. Kinase reactions were carried out using MBP as substrate with 0.15  $\mu$ M of purified human TNIK and 10  $\mu$ M peptides with or without a TNIK pre-autophosphorylation step. **(c)** Summary of DISC1 peptide effects. MBP phosphorylation in each reaction was normalized to the reaction with Tat peptide but without pre-autophosphorylation (lane 2). **(d)** DISCpep-WT inhibits kinase activity of endogenous TNIK. Kinase reactions were carried out using MBP as substrate with endogenous TNIK immunoprecipitated from HEK293 cells or 22 DIV rat hippocampal cultures (top) and 10  $\mu$ M of indicated peptides. The kinase input for each reaction was shown by western blotting using an anti-TNIK antibody (middle) and MBP input by Coomassie blue staining (bottom). **(e)** Summary of DISCpep-WT effect on endogenous TNIK. MBP phosphorylation in each reaction was normalized to the reaction with Tat peptide and TNIK from HEK293 cells.  $N = 3$ . \* $P < 0.05$ , \*\* $P < 0.01$ , \*\*\* $P < 0.001$ .

endogenous substrate(s) of TNIK are currently unknown, thus precluding the direct assessment of TNIK kinase activity. In addition, although TNIK

contains multiple phosphorylation sites throughout its 1360 amino acids (data not shown), the identity of possible residues that might act as markers of kinase

activity are unknown as well. We therefore used two commercially available TNIK phospho-antibodies against pSer764 and pSer769, which are phosphorylation sites identified by proteomic studies of the human kinome.<sup>42,43</sup> The specificity of these two antibodies was confirmed by western blot analysis of lysates expressing TNIK or TNIK AS mutants at these residues (Supplementary Figure 7a). Although phosphorylation of either serine is not required for MBP phosphorylation *in vitro* (Supplementary Figures 7b and c), glutamate receptor agonists and kinase activators actively regulate the phosphorylation of these two sites (Supplementary Figure 7d). Treatment of cells with DISCpep-WT-tat caused a marked decrease (about 50%) in the phosphorylation of TNIK at residues Ser764 and Ser769 (Figure 5a). To our surprise, however, such treatment also caused a marked reduction in total TNIK protein level (decreased by ~50% within 40 min treatment of DISCpep-WT-tat). In contrast, the control DISCpep-PM-tat peptide only showed a marginal decrease in the phosphorylation of Ser769, but had no effect on the total TNIK level and phosphorylation of Ser764 (Figure 5a).

In parallel, filamentous-to-globular-actin ratio was increased with DISCpep-WT-tat treatment (Figure 5b).

This effect is likely because of inhibition of TNIK, as overexpression of TNIK in HEK293 cells has been shown to induce actin depolymerization and decrease the filamentous-to-globular-actin ratio.<sup>30</sup> DISCpep-WT-tat also induced the rapid translocation of TNIK and actin from cytosolic to membrane fractions within 10 min of DISCpep-WT-tat treatment (Supplementary Figure 8). Importantly, control peptides had marginal or no activity on such effects (Figure 5b, Supplementary Figure 8).

Together, these data suggest that the DISCpep-WT-tat peptide specifically inhibits TNIK in primary hippocampal cultures likely by regulating both the absolute level of TNIK protein and its intrinsic kinase activity.

#### *Inhibition of TNIK leads to specific decreases of key PSD proteins*

We have previously shown that TNIK and DISC1 are localized and enriched at the PSD (Figures 2c–e). In addition, the total protein level and phosphorylation of TNIK are actively regulated in primary hippocampal cultures after treatment with glutamate receptor agonists or kinase-activating drugs (Supplementary Figure 7d). Together, these data suggested that TNIK

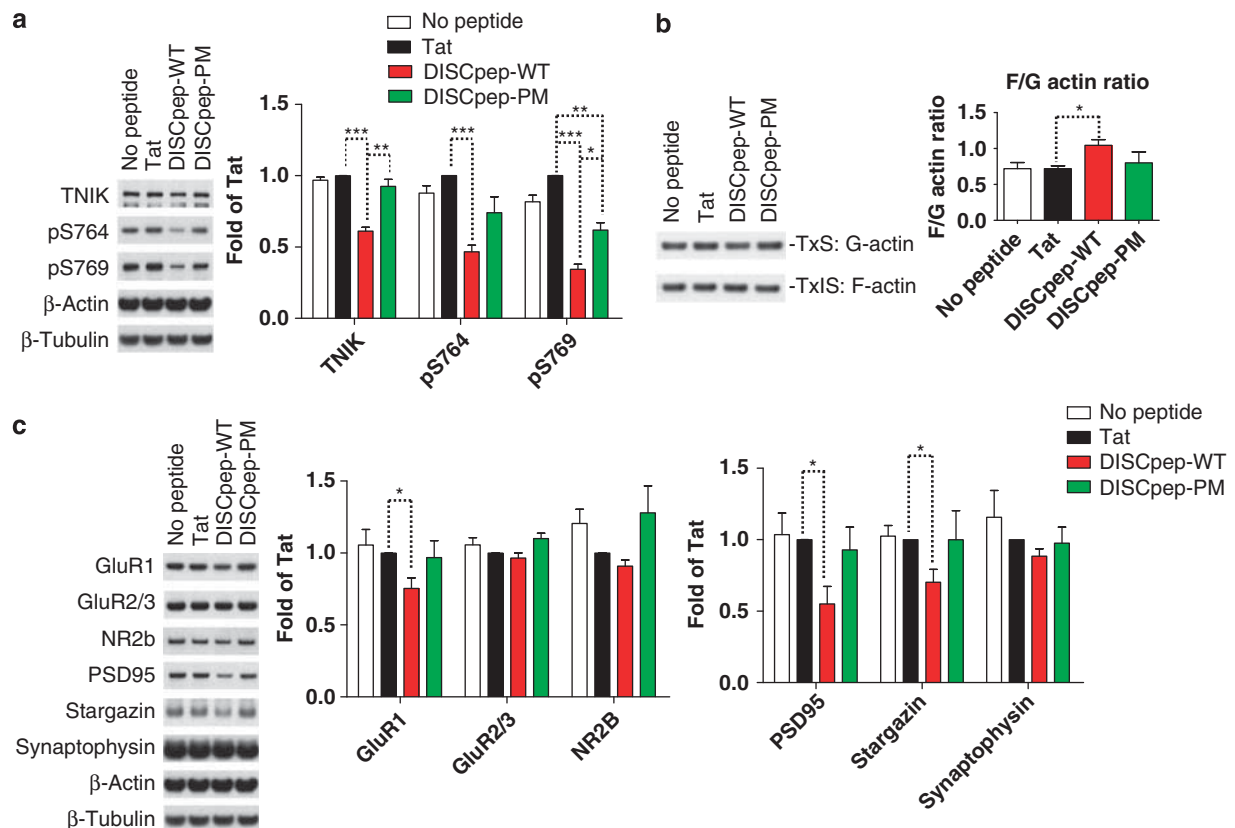


**Figure 5** DISC1-derived peptide inhibits TNIK and regulates levels of PSD proteins in primary hippocampal neurons. **(a)** DISCpep-WT causes a reduction in total TNIK and phospho-TNIK levels. Primary hippocampal neurons (16–22 DIV) were treated with 10  $\mu$ M of indicated peptides for 40 min.  $N=3$ . **(b)** DISCpep-WT increases the filamentous-to-globular (F/G)-actin ratio. Cultures were treated as in **(a)**, followed by Triton X-100 extraction to separate Triton soluble (TxS) and Triton insoluble (TxIS) fractions. TxS and TxIS contain G- and F-actin, respectively.<sup>30</sup>  $N=3$ . **(c)** DISCpep-WT causes a reduction in total levels of key PSD proteins. Peptide treatment was same as **(a)** except indicated proteins were analyzed.  $N=3$ . Total protein was normalized to  $\beta$ -actin, and phosphorylated protein to corresponding total protein. \* $P < 0.05$ , \*\* $P < 0.01$ , \*\*\* $P < 0.001$ .

might have a crucial role in signal transduction events during neuronal activation at the synapse, leading us to examine the consequence of TNIK inhibition by DISC<sub>pep</sub>-WT-tat on key synaptic proteins. Strikingly, within 40 min of treatment with DISC<sub>pep</sub>-WT-tat, the total protein levels of the AMPA receptor subunit GluR1, the transmembrane AMPA receptor regulatory protein stargazin, and the PSD scaffold protein PSD-95 were all dramatically decreased (Figure 5c). Interestingly, the dynamic interaction of these three molecules is important for the trafficking and function of AMPA receptors at the synapse.<sup>44–47</sup> Other AMPA receptor subunits (GluR2/3), the *N*-methyl *D*-aspartate receptor subunit NR2B and the presynaptic protein synaptophysin were not changed with the peptide treatment over the 40 min time range (Figure 5c). In addition, this specific effect of the DISC<sub>pep</sub>-WT-tat peptide was dose dependent and consistent between both primary hippocampal and cortical cultures (Supplementary Figure 9).

To understand the time course of the protein loss with the DISC<sub>pep</sub>-WT-tat peptide, we measured protein levels after 5, 10, 20 and 40 min of treatment. Dephosphorylation of TNIK and decreases in PSD-95 were observed at 5 min, suggesting that TNIK inhibition induces a rapid signaling cascade leading to protein degradation (Supplementary Figure 10). Furthermore, over the 40-min time course, there was good separation in the effects of DISC<sub>pep</sub>-WT-tat from the control peptide DISC<sub>pep</sub>-PM-tat, on inducing decreases in TNIK, GluR1, PSD-95 and stargazin (Supplementary Figure 10). Together, these results

suggest that TNIK activity is required to maintain the level of key synaptic proteins, with inhibition of TNIK resulting in a rapid depletion of these proteins.

#### Inhibition of TNIK induces degradation of PSD proteins

The reduction in GluR1 and PSD-95 protein levels occurs within minutes of DISC<sub>pep</sub>-WT treatment, leading us to hypothesize that inhibition of TNIK in this manner might selectively increase protein degradation rates. To test this hypothesis, primary hippocampal cultures were treated with the proteasome inhibitor MG132, or the lysosome inhibitor leupeptin, before treatment with Tat peptides. The reduction in TNIK protein levels induced by DISC<sub>pep</sub>-WT-tat was rescued by MG132 but not leupeptin. However, dephosphorylation of TNIK at S764 was not affected by MG132, and S769 was neither affected by MG132 or leupeptin treatments (Figures 6a and b). This suggests that DISC<sub>pep</sub>-WT-tat still alters TNIK phosphorylation status in the presence of MG132 or leupeptin. Critically, the loss of PSD-95 protein was blocked by MG132, but not leupeptin, with a reciprocal effect observed for GluR1 (Figures 6a and b). The degradative pathways implied from these data are consistent with the cytoplasmic protein PSD-95 being degraded through the proteasome, and the transmembrane receptor GluR1 through the lysosome.<sup>48,49</sup> These results suggest that TNIK is a critical signaling molecule at the synapse that protects specific postsynaptic proteins, such as PSD-95 and GluR1, from degradation.

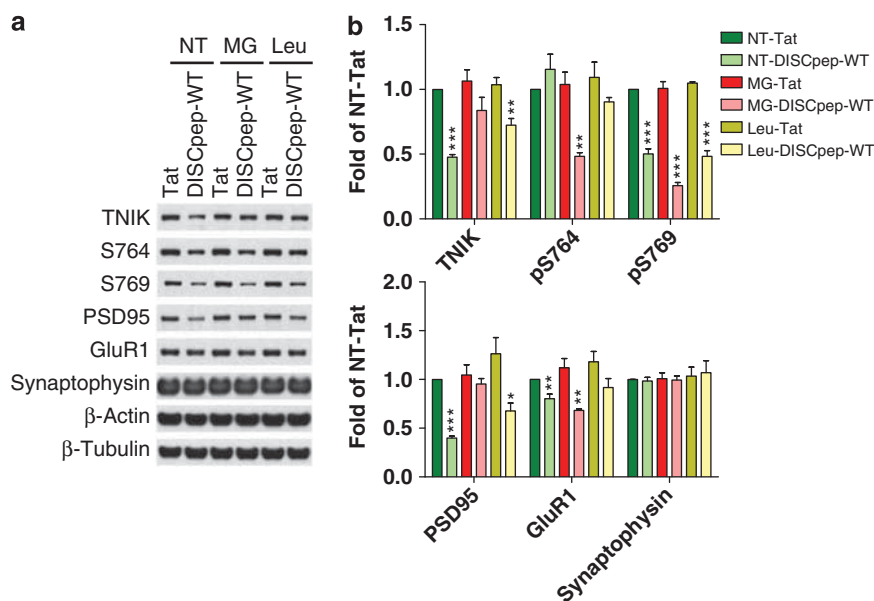


**Figure 6** Loss of PSD95 and GluR1 after inhibition of TNIK is through proteasomal and lysosomal degradation pathways. (a) Degradation of PSD-95 and GluR1 was rescued by the proteasome inhibitor, MG132, and the lysosome inhibitor, leupeptin, respectively. Primary hippocampal neurons (16–22 DIV) were pretreated with 10  $\mu$ M of MG132 or 25  $\mu$ g ml<sup>-1</sup> of leupeptin for 7 h before treatment with 10  $\mu$ M of the indicated peptide for 40 min. (b) Summary of the effects of MG132 and leupeptin. *N*=4. Total protein was normalized to  $\beta$ -actin, and phosphorylated protein to corresponding total protein. \**P*<0.05, \*\**P*<0.01, \*\*\**P*<0.001.

### *Inhibition of TNIK leads to decreases in surface GluR1 and AMPA receptor currents*

To determine whether the observed degradation of PSD proteins occurred at synapses, immunofluorescence staining was performed on hippocampal neurons after 30 min of treatment with the various Tat peptides. Treatment with DISCpep-WT-tat specifically decreased both the size and total intensity of surface GluR1 and PSD-95 immunoreactive puncta per 50  $\mu\text{m}$  of dendrite in comparison to both DISCpep-PM and tat alone (Figures 7a and b and Supplementary Figure 11). The puncta density of surface GluR1 along dendrites was also decreased in comparison to both control peptides, whereas there was a more modest effect on PSD95 puncta density with significance over DISCpep-PM but not tat. Consistent with these imaging data, we were able to record decreases in amplitude and frequency of isolated AMPA receptor mEPSCs in primary hippocampal neurons after treatment with DISCpep-WT-tat (Figure 7c). Together, these results suggest that not only does inhibition of TNIK lead to reductions in the total protein levels of GluR1 and PSD95, but it also reduces their level at the synapse and reduces synaptic strength.

### *DISC1 and TNIK regulate AMPA receptors in a reciprocal but complex manner*

The DISCpep-WT-tat peptide experiments suggest that TNIK has an important role in the life cycle of a number of PSD proteins. To gain additional data to support these observations, we developed lentiviral-expressed shRNA reagents to knock down TNIK expression levels. We characterized two independent shRNA constructs (shRNAs 806 and 807) directed against distinct sequences of TNIK, which reduced expression levels of overexpressed mouse/rat TNIK in HEK293 cells (Supplementary Figure 12a). Moreover, both shRNAs effectively knocked down endogenous TNIK levels in primary hippocampal cultures 14 days after virus transduction (Supplementary Figures 12b and c). We used the more potent virus shRNA-807 in all further experiments, together with the control empty virus 801 (named TNIK RNAi and ctrl RNAi) to demonstrate the effects of knocking down TNIK levels. Thus, we evaluated the effects of TNIK knockdown on the same set of PSD proteins as analyzed above for the peptide experiments. Intriguingly, and in contrast to the peptide experiments, all PSD proteins tested, including GluR1, GluR2/3, NR2B, PSD-95 and stargazin, were reduced by TNIK knockdown, whereas the presynaptic protein synaptophysin was unchanged (Figures 8a and b). Such

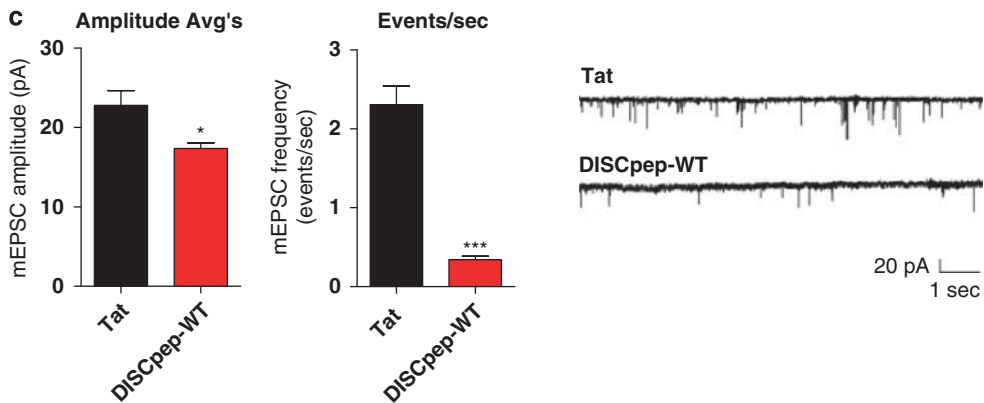
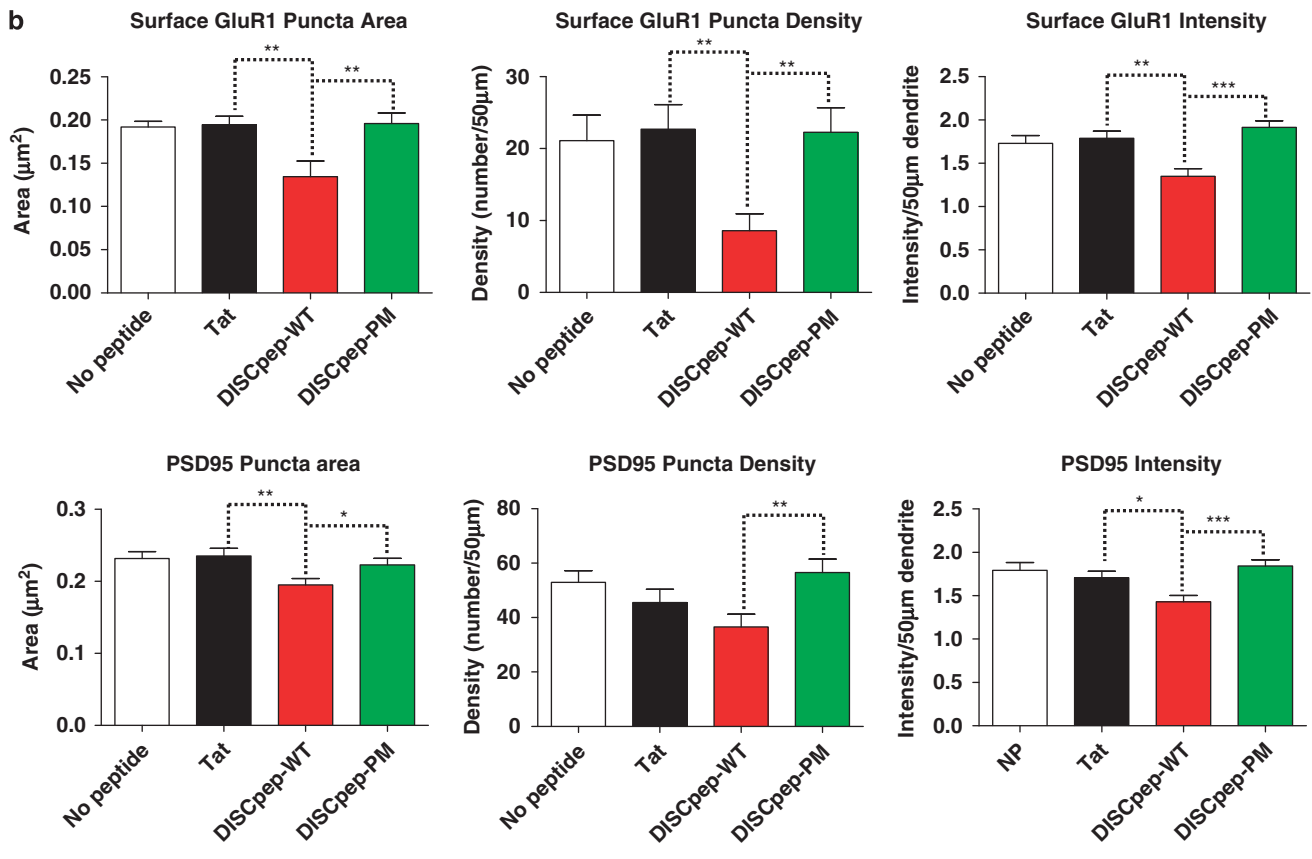
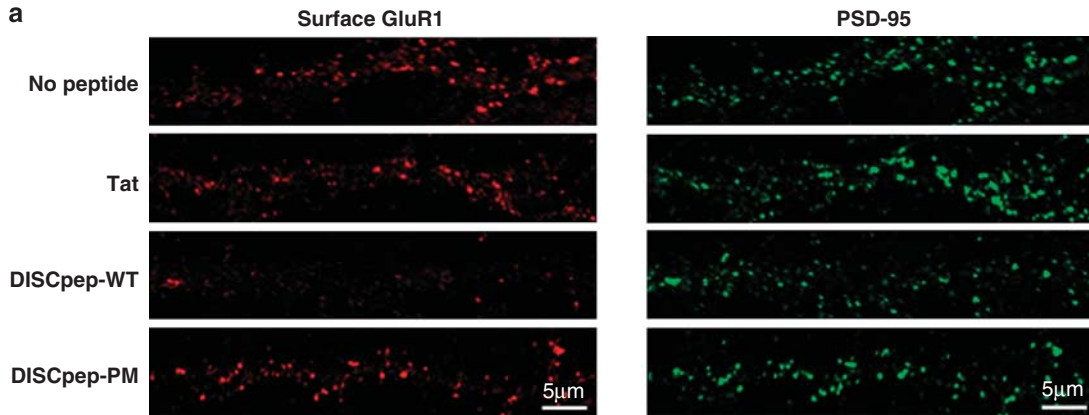
differences could be because of the different approaches taken (kinase inhibition versus protein depletion) or because of the time course of the experiments (chronic knockdown versus acute kinase inhibition). TNIK knockdown also resulted in reduced surface levels of GluR1 as measured by pull-down of biotinylated surface proteins (Figures 8c and d). Consistent with this, the amplitude of isolated AMPA receptor mEPSCs was decreased with TNIK knockdown. Critically, this decrease could be rescued by co-transfection of a knockdown-resistant TNIK construct, but not by wild-type TNIK (Figure 8e and Supplementary Figure 12a). The effects of TNIK knockdown support the suggested role of TNIK in the maintenance of PSD protein stability.

As DISC1 binds TNIK in the PSD and is an inhibitor of TNIK kinase activity, we set out to evaluate the effect of DISC1 knockdown on the pool of proteins regulated by TNIK activity. We hypothesized that depletion of DISC1 should lead to an elevation in TNIK activity and hence a phenotype reciprocal to that observed with either TNIK knockdown or use of the DISC1 inhibitory peptide, DISCpep-WT-tat. Indeed, DISC1 knockdown, using a well-characterized shRNA lentivirus,<sup>19,39</sup> caused an increase in GluR1 and GluR2/3 (Figure 8f). DISC1 knockdown also led to an increase in the level of TNIK protein, suggesting that not only does DISC1 regulate the activity of TNIK but also its degradation (Figure 8f). DISC1 knockdown also reduced levels of PSD-95 and stargazin (Figure 8f). These latter effects may be explained by the effects of DISC1 depletion on other DISC1 interactors and functions.<sup>11,26</sup> Together, these data indicate that the DISC1–TNIK interaction regulates glutamate receptors and other critical PSD proteins in a dynamic fashion.

## Discussion

Changes in the molecular composition and signaling properties of the PSD serve as an important mechanism to alter synaptic strength, which is thought to underlie information storage and learning-related plasticity,<sup>50,51</sup> whereas deficits in synaptic form and function are now considered primary molecular insults that lead to a range of psychiatric and neurological disorders. This study identifies the DISC1–TNIK complex, a combination of two emerging disease risk factors, as a new molecular player at excitatory synapses. We demonstrate for the first time that TNIK maintains levels of glutamate receptors and other key PSD proteins at the synapse, with loss of TNIK protein or inhibition of TNIK activity causing

**Figure 7** Inhibition of TNIK leads to decreases in both the surface levels of GluR1 and AMPAR mEPSCs. **(a)** Representative images of dendritic segments of primary hippocampal neurons (19–22 DIV) treated with 10  $\mu\text{M}$  of indicated peptide for 30 min, followed by immunostaining for surface GluR1 and PSD-95. **(b)** DISCpep-WT treatment decreases the size, density and intensity of the surface GluR1 and PSD-95 puncta.  $N = 15$ . **(c)** DISCpep-WT treatment decreases both mEPSC amplitude and frequency of primary hippocampal neurons (13 or 19 DIV) pretreated for 40 min with indicated peptides. Representative traces are shown on the right.  $N \geq 4$ . \* $P < 0.05$ , \*\* $P < 0.01$ , \*\*\* $P < 0.001$ .



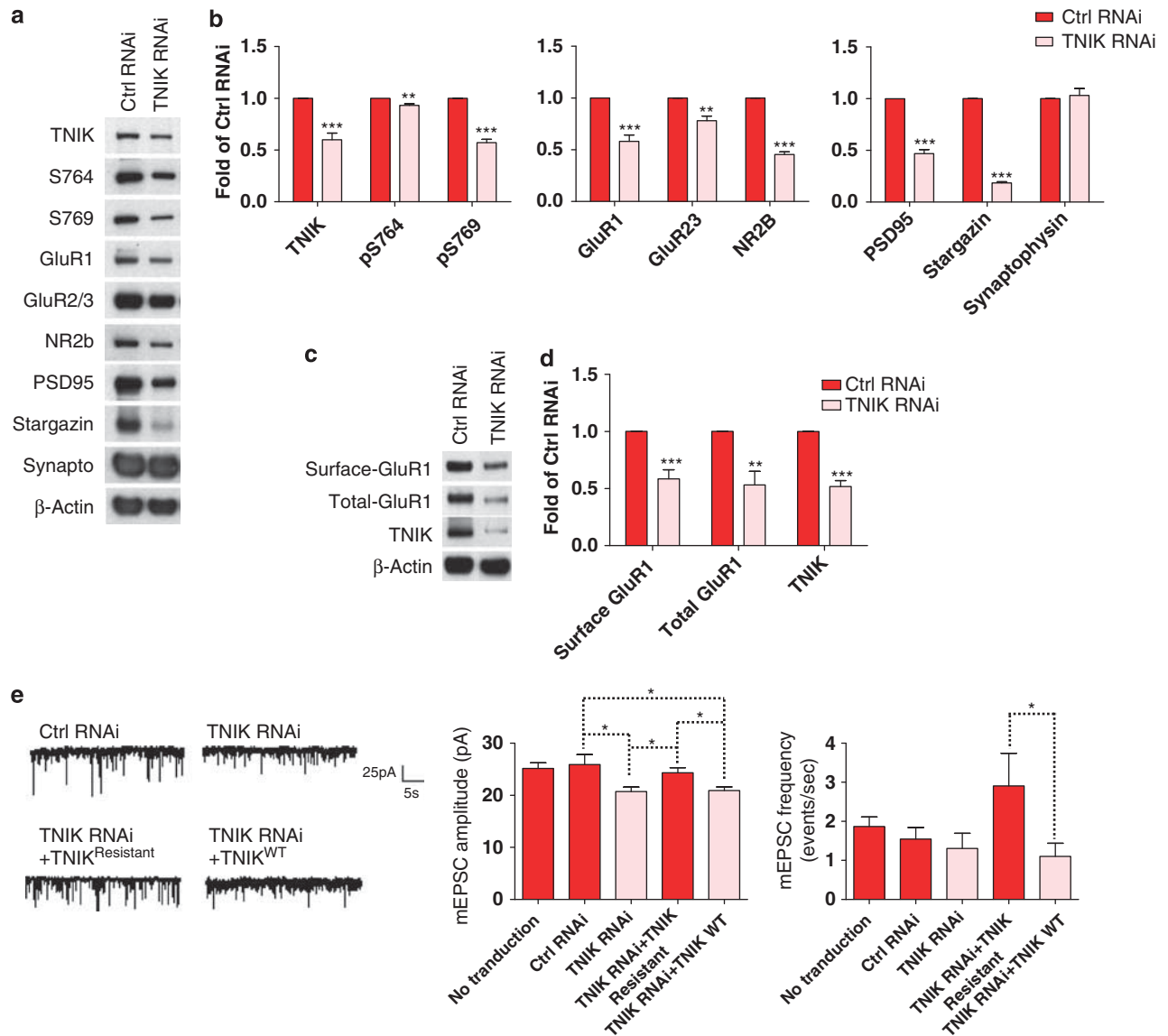


**Figure 8** DISC1 and TNIK regulate components of the PSD in a complex fashion. (a, b) TNIK knockdown by a lentiviral-expressed shRNA regulates the level of PSD proteins in primary hippocampal cultures consistent with effects mediated by peptide inhibition.  $N=4$ . (c, d) TNIK shRNA knockdown causes decreases in total and surface GluR1.  $N=5$ . (e) TNIK shRNA knockdown causes decreases in mEPSC amplitude, but not frequency, in primary hippocampal neurons, and this decrease can be rescued by knockdown-resistant TNIK but not by WT TNIK. The representative traces are shown on the right.  $N \geq 4$ . (f) DISC1 knockdown regulates the level of PSD proteins in primary hippocampal cultures.  $N=3$ . Total protein was normalized to  $\beta$ -actin, and phosphorylated protein to corresponding total protein. \* $P < 0.05$ , \*\* $P < 0.01$ , \*\*\* $P < 0.001$ .

rapid degradation of PSD constituents. DISC1 appears to be a key cellular brake for TNIK activity as (1) in a cellular overexpression system, DISC1 inhibits TNIK activity in a manner that is dependent on DISC1 binding to TNIK (Figure 3) and (2) a peptide derived from the TNIK binding site on DISC1 (DISC1<sup>pep</sup>-WT-tat) inhibits TNIK kinase activity and leads to the degradation of postsynaptic proteins in hippocampal neurons (Figures 4–6). In addition, this treatment also resulted in a loss of AMPAR GluR1 surface staining at synapses and a reduction in AMPAR mEPSCs (Figure 7). Together, these data suggest that regulation of TNIK activity either directly, or indir-

ectly through DISC1, can modulate synaptic strength. Intriguingly, inhibition of TNIK with the peptide DISC1<sup>pep</sup>-WT also led to a reduction in total protein levels of TNIK that could account for some of the effects we see on postsynaptic proteins, as mimicked by the shRNA experiments. It is critical to note that in primary cultures treated with MG132 and subsequent DISC1<sup>pep</sup>-WT-tat, GluR1 degradation still occurred, although the total protein loss of TNIK was rescued by MG132 (Figures 6a and b), suggesting that the kinase activity of TNIK, probably regulated by phosphorylation, is required for the maintenance of some PSD proteins.

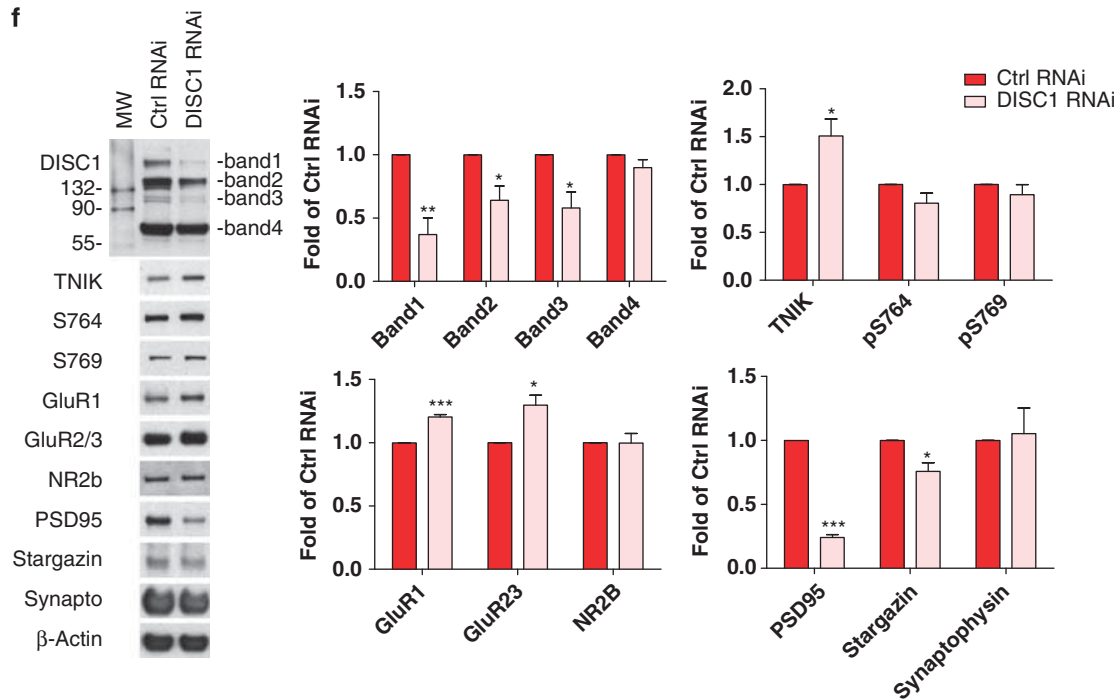


**Figure 8** Continued.

The importance of TNIK in regulating components of the PSD was reinforced by knocking down TNIK using shRNAs. We again saw a decrease in a range of PSD proteins, accompanied by decreases in GluR1 surface expression and AMPAR currents (Figure 8). Intriguingly, when we knocked down DISC1, we saw a partially reciprocal set of protein changes as seen with TNIK knockdown. We observed predicted increases in the levels of TNIK and GluR1 but surprisingly a very large decrease in PSD-95 levels. This latter finding, which did not fit our hypothesis, might be explained by effects of DISC1 loss on other PSD-localized DISC1 complexes.<sup>26</sup> In particular, the interaction between kalirin-7 and DISC1 may be relevant for this effect. Indeed, in a separate study we have recently shown that DISC1 binds to kal-7 and PSD-95 in a tri-molecular signalosome, to prevent access of kal-7 to rac1 and regulate spine size.<sup>39</sup> It is possible that depletion of DISC1 from the kal-7 pool may destabilize PSD-95 and mask possible increases resulting from a disinhibition of TNIK. Consequently, it is now vital to understand the function of the DISC1–TNIK interaction at the synapse within the context of other DISC1-interacting proteins, in particular kal-7. Knowledge of the downstream signaling pathways from TNIK and kal-7 identifies convergence at the level of regulation of the actin cytoskeleton.<sup>52</sup> It is now critical to understand whether these effects are independent or possibly components of a single linear pathway. Intriguingly, we show that TNIK is regulated by *N*-methyl D-aspartate receptor activation (Supplementary Figure 7d), which has also been shown to regulate the complex of DISC1, kal-7 and PSD-95.<sup>39</sup> Again, whether TNIK activity might have a

role in the formation and stabilization of this tri-partite complex awaits additional studies. In addition, a number of other DISC1 partners are localized to the synapse, for example, PDE4,<sup>53</sup> but we believe that the effects we observe with the DISC1pep-WT peptide are specific to TNIK, as the TNIK binding site does not overlap with known binding sites of other DISC1 interactors, including PDE4, NUDEL, Grb2, glycogen synthase kinase-3 $\beta$  and Girdin,<sup>17,20,21,54–56</sup> and the effects we are observing are likely to be through inhibition of kinase activity rather than through disruption of protein–protein interactions. We do not yet understand the downstream effectors of TNIK kinase activity that are responsible for regulating PSD protein degradation. We are currently identifying TNIK substrates, but do not have likely candidate(s) that would explain the data reported here. Previous studies highlighted the importance of TNIK in regulating the actin cytoskeleton,<sup>30,31</sup> and we speculate that actin regulatory proteins could be important targets. This possibility is supported by our demonstration that DISC1 inhibits TNIK-induced cell rounding, an actin-dependent process, in HEK293 cells, and that inhibiting TNIK by the DISC1pep-WT peptide induces the translocation of actin from the cytosol to the membrane and increases the filamentous-to-globular-actin ratio in primary hippocampal cultures (Figures 3 and 5b and Supplementary Figure 8). It is not clear that these TNIK–actin events have a role in TNIK regulation of PSD proteins. However, actin is highly enriched at the PSD, where it anchors receptors and regulates receptor trafficking,<sup>57</sup> enabling TNIK to synergistically regulate the composition and structure of dendritic spines.

In conclusion, we show that TNIK and DISC1 are key regulators of components of the PSD and consequently of synapse form and function. As deficits in synaptic function are implicated in diseases like autism and schizophrenia, a deeper molecular understanding of risk factors like DISC1 has the potential to create new opportunities for understanding and treating these diseases.

### Conflict of interest

The authors declare no conflict of interest.

### Acknowledgments

We thank Drs Carsten Korth, Hongjun Song and Atsushi Kamiya for reagents and scientific discussion. We thank Dr Pranab Chanda, Annette Sievers, Lora Cameron-Landis, Xiaotian Zhong and Adarsh Godbole for assistance in protein purification.

### References

- Pardo CA, Eberhart CG. The neurobiology of autism. *Brain Pathol* 2007; **17**: 434–447.
- Sanacora G, Zarate CA, Krystal JH, Manji HK. Targeting the glutamatergic system to develop novel, improved therapeutics for mood disorders. *Nat Rev Drug Discov* 2008; **7**: 426–437.
- Sodhi M, Wood KH, Meador-Woodruff J. Role of glutamate in schizophrenia: integrating excitatory avenues of research. *Expert Rev Neurother* 2008; **8**: 1389–1406.
- Coyle JT. Glutamate and schizophrenia: beyond the dopamine hypothesis. *Cell Mol Neurobiol* 2006; **26**: 365–384.
- Schiffer HH. Glutamate receptor genes: susceptibility factors in schizophrenia and depressive disorders? *Mol Neurobiol* 2002; **25**: 191–212.
- Meador-Woodruff JH, Healy DJ. Glutamate receptor expression in schizophrenic brain. *Brain Res Brain Res Rev* 2000; **31**: 288–294.
- Ohnuma T, Kato H, Arai H, Faull RL, McKenna PJ, Emson PC. Gene expression of PSD95 in prefrontal cortex and hippocampus in schizophrenia. *NeuroReport* 2000; **11**: 3133–3137.
- Mirnics K, Middleton FA, Lewis DA, Levitt P. Analysis of complex brain disorders with gene expression microarrays: schizophrenia as a disease of the synapse. *Trends Neurosci* 2001; **24**: 479–486.
- Pennington K, Beasley CL, Dicker P, Fagan A, English J, Pariante CM *et al*. Prominent synaptic and metabolic abnormalities revealed by proteomic analysis of the dorsolateral prefrontal cortex in schizophrenia and bipolar disorder. *Mol Psychiatry* 2008; **13**: 1102–1117.
- Chubb JE, Bradshaw NJ, Soares DC, Porteous DJ, Millar JK. The DISC locus in psychiatric illness. *Mol Psychiatry* 2008; **13**: 36–64.
- Brandon NJ, Millar JK, Korth C, Sive H, Singh KK, Sawa A. Understanding the role of DISC1 in psychiatric disease and during normal development. *J Neurosci* 2009; **29**: 12768–12775.
- Millar JK, Wilson-Annan JC, Anderson S, Christie S, Taylor MS, Semple CA *et al*. Disruption of two novel genes by a translocation co-segregating with schizophrenia. *Hum Mol Genet* 2000; **9**: 1415–1423.
- St Clair D, Blackwood D, Muir W, Carothers A, Walker M, Spowart G *et al*. Association within a family of a balanced autosomal translocation with major mental illness. *Lancet* 1990; **336**: 13–16.
- Millar JK, Christie S, Anderson S, Lawson D, Hsiao-Wei Loh D, Devon RS *et al*. Genomic structure and localisation within a linkage hotspot of disrupted in schizophrenia 1, a gene disrupted by a translocation segregating with schizophrenia. *Mol Psychiatry* 2001; **6**: 173–178.
- Wang Q, Jaaro-Peled H, Sawa A, Brandon NJ. How has DISC1 enabled drug discovery? *Mol Cell Neurosci* 2008; **37**: 187–195.
- Millar JK, Pickard BS, Mackie S, James R, Christie S, Buchanan SR *et al*. DISC1 and PDE4B are interacting genetic factors in schizophrenia that regulate cAMP signaling. *Science* 2005; **310**: 1187–1191.
- Murdoch H, Mackie S, Collins DM, Hill EV, Bolger GB, Klusmann E *et al*. Isoform-selective susceptibility of DISC1/phosphodiesterase-4 complexes to dissociation by elevated intracellular cAMP levels. *J Neurosci* 2007; **27**: 9513–9524.
- Jaaro-Peled H, Hayashi-Takagi A, Seshadri S, Kamiya A, Brandon NJ, Sawa A. Neurodevelopmental mechanisms of schizophrenia: understanding disturbed postnatal brain maturation through neuregulin-1-ErbB4 and DISC1. *Trends Neurosci* 2009; **32**: 485–495.
- Kamiya A, Kubo K, Tomoda T, Takaki M, Youn R, Ozeki Y *et al*. A schizophrenia-associated mutation of DISC1 perturbs cerebral cortex development. *Nat Cell Biol* 2005; **7**: 1167–1178.
- Kim JY, Duan X, Liu CY, Jang MH, Guo JU, Pow-anpongkul N *et al*. DISC1 regulates new neuron development in the adult brain via modulation of AKT-mTOR signaling through KIAA1212. *Neuron* 2009; **63**: 761–773.
- Mao Y, Ge X, Frank CL, Madison JM, Koehler AN, Doud MK *et al*. Disrupted in schizophrenia 1 regulates neuronal progenitor proliferation via modulation of GSK3beta/beta-catenin signaling. *Cell* 2009; **136**: 1017–1031.
- Taya S, Shinoda T, Tsuboi D, Asaki J, Nagai K, Hikita T *et al*. DISC1 regulates the transport of the NUDEL/LIS1/14-3-3epsilon complex through kinesin-1. *J Neurosci* 2007; **27**: 15–26.
- Bradshaw NJ, Ogawa F, Antolin-Fontes B, Chubb JE, Carlyle BC, Christie S *et al*. DISC1, PDE4B, and NDE1 at the centrosome and synapse. *Biochem Biophys Res Commun* 2008; **377**: 1091–1096.
- Clapcote SJ, Lipina TV, Millar JK, Mackie S, Christie S, Ogawa F *et al*. Behavioral phenotypes of Disc1 missense mutations in mice. *Neuron* 2007; **54**: 387–402.
- Kirkpatrick B, Xu L, Cascella N, Ozeki Y, Sawa A, Roberts RC. DISC1 immunoreactivity at the light and ultrastructural level in the human neocortex. *J Comp Neurol* 2006; **497**: 436–450.
- Camargo LM, Collura V, Rain JC, Mizuguchi K, Hermjakob H, Kerrien S *et al*. Disrupted in schizophrenia 1 interactome: evidence for the close connectivity of risk genes and a potential synaptic basis for schizophrenia. *Mol Psychiatry* 2007; **12**: 74–86.
- Brandon NJ. Dissecting DISC1 function through protein-protein interactions. *Biochem Soc Trans* 2007; **35**(Part 5): 1283–1286.
- Collins MO, Yu L, Coba MP, Husi H, Campuzano I, Blackstock WP *et al*. Proteomic analysis of in vivo phosphorylated synaptic proteins. *J Biol Chem* 2005; **280**: 5972–5982.
- Peng J, Kim MJ, Cheng D, Duong DM, Gygi SP, Sheng M. Semiquantitative proteomic analysis of rat forebrain postsynaptic density fractions by mass spectrometry. *J Biol Chem* 2004; **279**: 21003–21011.
- Fu CA, Shen M, Huang BC, Lasaga J, Payan DG, Luo Y. TNIK, a novel member of the germinal center kinase family that activates the c-Jun N-terminal kinase pathway and regulates the cytoskeleton. *J Biol Chem* 1999; **274**: 30729–30737.
- Taira K, Umikawa M, Takei K, Myagmar BE, Shinzato M, Machida N *et al*. The Traf2- and Nck-interacting kinase as a putative effector of Rap2 to regulate actin cytoskeleton. *J Biol Chem* 2004; **279**: 49488–49496.
- Mahmoudi T, Li VS, Ng SS, Taouatas N, Vries RG, Mohammed S *et al*. The kinase TNIK is an essential activator of Wnt target genes. *EMBO J* 2009; **28**: 3329–3340.
- Glatt SJ, Everall IP, Kremen WS, Corbeil J, Sasik R, Khanlou N *et al*. Comparative gene expression analysis of blood and brain provides concurrent validation of SELENBP1 up-regulation in schizophrenia. *Proc Natl Acad Sci USA* 2005; **102**: 15533–15538.
- Matigian N, Windus L, Smith H, Filippich C, Pantelis C, McGrath J *et al*. Expression profiling in monozygotic twins discordant for bipolar disorder reveals dysregulation of the WNT signalling pathway. *Mol Psychiatry* 2007; **12**: 815–825.
- Potkin SG, Turner JA, Guffanti G, Lakatos A, Fallon JH, Nguyen DD *et al*. A genome-wide association study of schizophrenia using brain activation as a quantitative phenotype. *Schizophr Bull* 2009; **35**: 96–108.
- Shi J, Levinson DF, Duan J, Sanders AR, Zheng Y, Pe'er I *et al*. Common variants on chromosome 6p22.1 are associated with schizophrenia. *Nature* 2009; **460**: 753–757.

- 37 Banker GA, Cowan WM. Rat hippocampal neurons in dispersed cell culture. *Brain Res* 1977; **126**: 397–425.
- 38 Kamiya A, Tomoda T, Chang J, Takaki M, Zhan C, Morita M *et al*. DISC1-NDEL1/NUDEL protein interaction, an essential component for neurite outgrowth, is modulated by genetic variations of DISC1. *Hum Mol Genet* 2006; **15**: 3313–3323.
- 39 Hayashi-Takagi A, Takaki M, Graziane N, Seshadri S, Murdoch H, Dunlop AJ *et al*. Disrupted-in-schizophrenia 1 (DISC1) regulates spines of the glutamate synapse via Rac1. *Nat Neurosci* 2010; **13**: 327–332.
- 40 Nonaka H, Takei K, Umikawa M, Oshiro M, Kuninaka K, Bayarjargal M *et al*. MINK is a Rap2 effector for phosphorylation of the postsynaptic scaffold protein TANC1. *Biochem Biophys Res Commun* 2008; **377**: 573–578.
- 41 Brandon NJ, Schurov I, Camargo LM, Handford EJ, Duran-Jimenez B, Hunt P *et al*. Subcellular targeting of DISC1 is dependent on a domain independent from the Nudel binding site. *Mol Cell Neurosci* 2005; **28**: 613–624.
- 42 Shu H, Chen S, Bi Q, Mumby M, Brekken DL. Identification of phosphoproteins and their phosphorylation sites in the WEHI-231 B lymphoma cell line. *Mol Cell Proteomics* 2004; **3**: 279–286.
- 43 Oppermann FS, Gnad F, Olsen JV, Hornberger R, Greff Z, Keri G *et al*. Large-scale proteomics analysis of the human kinome. *Mol Cell Proteomics* 2009; **8**: 1751–1764.
- 44 Tomita S, Fukata M, Nicoll RA, Brecht DS. Dynamic interaction of stargazin-like TARPs with cycling AMPA receptors at synapses. *Science* 2004; **303**: 1508–1511.
- 45 Chen L, Chetkovich DM, Petralia RS, Sweeney NT, Kawasaki Y, Wenthold RJ *et al*. Stargazin regulates synaptic targeting of AMPA receptors by two distinct mechanisms. *Nature* 2000; **408**: 936–943.
- 46 Tomita S, Adesnik H, Sekiguchi M, Zhang W, Wada K, Howe JR *et al*. Stargazin modulates AMPA receptor gating and trafficking by distinct domains. *Nature* 2005; **435**: 1052–1058.
- 47 Bats C, Groc L, Choquet D. The interaction between Stargazin and PSD-95 regulates AMPA receptor surface trafficking. *Neuron* 2007; **53**: 719–734.
- 48 Colledge M, Snyder EM, Crozier RA, Soderling JA, Jin Y, Langeberg LK *et al*. Ubiquitination regulates PSD-95 degradation and AMPA receptor surface expression. *Neuron* 2003; **40**: 595–607.
- 49 Ehlers MD. Reinsertion or degradation of AMPA receptors determined by activity-dependent endocytic sorting. *Neuron* 2000; **28**: 511–525.
- 50 Newpher TM, Ehlers MD. Spine microdomains for postsynaptic signaling and plasticity. *Trends Cell Biol* 2009; **19**: 218–227.
- 51 Kasai H, Fukuda M, Watanabe S, Hayashi-Takagi A, Noguchi J. Structural dynamics of dendritic spines in memory and cognition. *Trends Neurosci* 2010; **33**: 121–129.
- 52 Penzes P, Jones KA. Dendritic spine dynamics—a key role for kalirin-7. *Trends Neurosci* 2008; **31**: 419–427.
- 53 Collins DM, Murdoch H, Dunlop AJ, Charych E, Baillie GS, Wang Q *et al*. Ndel1 alters its conformation by sequestering cAMP-specific phosphodiesterase-4D3 (PDE4D3) in a manner that is dynamically regulated through protein kinase A (PKA). *Cell Signal* 2008; **20**: 2356–2369.
- 54 Brandon NJ, Handford EJ, Schurov I, Rain JC, Pelling M, Duran-Jimenez B *et al*. Disrupted in schizophrenia 1 and Nudel form a neurodevelopmentally regulated protein complex: implications for schizophrenia and other major neurological disorders. *Mol Cell Neurosci* 2004; **25**: 42–55.
- 55 Enomoto A, Asai N, Namba T, Wang Y, Kato T, Tanaka M *et al*. Roles of disrupted-in-schizophrenia 1-interacting protein girdin in postnatal development of the dentate gyrus. *Neuron* 2009; **63**: 774–787.
- 56 Shinoda T, Taya S, Tsuboi D, Hikita T, Matsuzawa R, Kuroda S *et al*. DISC1 regulates neurotrophin-induced axon elongation via interaction with Grb2. *J Neurosci* 2007; **27**: 4–14.
- 57 Cingolani LA, Goda Y. Actin in action: the interplay between the actin cytoskeleton and synaptic efficacy. *Nat Rev Neurosci* 2008; **9**: 344–356.

Supplementary Information accompanies the paper on the Molecular Psychiatry website (<http://www.nature.com/mp>)